



Norwegian University of
Science and Technology

Antenna for subsea communication in strong magnetic field

Lars-Arne Larsen

Master of Science in Electronics

Submission date: June 2016

Supervisor: Egil Eide, IET

Co-supervisor: Audun Andersen, Wireless Power & Communication AS

Norwegian University of Science and Technology
Department of Electronics and Telecommunications

Problem description

The student will perform a parametric study of the model created in the project [1] to get a more optimal configuration. The student will perform a literature study to evaluate a new antenna design. These new antenna designs will be verified using a model in CST and physical measurements. If there is enough time, the student will perform new measurements on the antennas mounted in the connector. The goal for this master's thesis is to design a new antenna where the transfer rate is higher than the original antenna (15Mbps).

Abstract

In subsea, it is difficult to create connectors for power transfer or communication, therefore Wireless Power & Communication (WPC) have created a wireless connector. The incentive for this connector is that metals do not last long exposed to the salt water, and a closed waterproof connector is advantageous. In this thesis, the focus is on a connector from WPC called 150W-RSE Subsea Connector, which is found in [2]. The goal for this thesis is to perform a parametric study of the antenna currently in use by WPC, and on a new design presented by the student. These parametric studies is then used to discuss how the properties of the antennas changes dependent on the different values and present a more optimal design for WPC to use. After some testing, it became apparent that the measurements were unstable because of a standing wave on the coax connecting the antennas. The results after connecting a 50 ohm resistor to the antennas were not compared to any simulations, but an increase in stability is noticeable. To conclude, the presented antennas were usable for transmission using the wifi-chip, but further testing with the actual connector with a resistor connected is recommended to increase the predictability and stability.

Sammendrag

Under vann er det en utfordring å lage konnektorer for overføring av effekt eller kommunikasjon. På grunn av denne utfordringen, har bedriften Wireless Power & Communications (WPC) laget en trådløs konektor. Motivasjonen bak denne konnektoren er det at metall fort blir ødelagt og korroderer bort i saltvann og en lukket vanntett konektor er ønsket. I denne oppgaven er fokuset på en konektor laget av WPC med navn 150W-RSE Subsea Connector som er funnet i [2]. Målet for oppgaven er å gjennomføre et parametrisk studie på antennen som blir brukt av WPC, og på en ny antenne foreslått av studenten. Disse to parametriske søkene blir diskutert for å bestemme hvordan de forskjellige parametrene påvirker frekvensresponsen til konnektoren og dermed foreslå en mer optimal løsning. Etter noen innledende målinger merkes det at målingene er meget ustabile og blir lett påvirket av eksterne påvirkninger som et resultat av en stående reflektert bølge på coaxial kablen. For å motvirke denne ustabiliteten, ble en 50 Ohms resistor tilkoblet antennene. Det ble ikke gjort noen simiuleringer for å sammenligne resultatene med modellen, men stabiliteten økte betraktelig. For å konkludere, begge antenntypene diskutert fungerer bra til å overføre ved hjelp av wifi-brikken brukt. Men det er anbefalt å gjennomføre nye målinger hvor antennen er satt i konnektoren og eventuelt forandre på parametrene for å forbedre stabiliteten.

Preface

This report is submitted as a master's thesis for the degree of Master Of Science (MSc) at the Norwegian University of Science and Technology (NTNU). The work was carried out in the period January to June 2015 under the supervision of adjunct associate professor Egil Eide (NTNU) and Audun Andersen, Managing Director at Wireless Power & Communications AS (WPC). The project was given by WPC to NTNU to study and, if possible, improve the wireless transfer rate of the antenna used for data communication in the connector 150W-RSE Subsea Connector shown in Figure 1-1 and found in [2].

The wireless transfer is done by using two chips of the type WizFi630 to create a wireless connection using the 2.4-2.483GHz band. The setup used today gives a transfer rate of 15Mbps [2]. By increasing the bandwidth available to 40MHz, it is possible to use the 802.11n standard, which should have a maximum transfer rate of 150Mbps [3].

Contents

ABSTRACT	II
SAMMENDRAG	III
PREFACE	IV
1 INTRODUCTION	1
1.1 MOTIVATION AND GOALS	1
2 THEORY AND LITERATURE RESEARCH	3
2.1 ANTENNA PARAMETERS	3
2.1.1 <i>Electric length</i>	3
2.1.2 <i>Near and far field</i>	3
2.1.3 <i>S-parameters</i>	5
2.1.4 <i>Forward Loss Factor</i>	6
2.2 ELECTRICALLY SHORT ANTENNAS	6
2.3 ORIGINAL ANTENNAS	7
2.4 NEW ANTENNAS	9
2.4.1 <i>Circular patch antenna</i>	9
2.4.2 <i>Open coaxial coupling antenna</i>	9
3 MODELS IN CST	17
3.1 EXPANDED MODEL	17
3.2 PARAMETRIC STUDY	17
3.2.1 <i>Original design antennas</i>	17
3.2.2 <i>Open coaxial antennas</i>	19
3.2.3 <i>Chosen antenna designs</i>	21
4 MEASUREMENTS	23
4.1 MEASUREMENT TECHNIQUES	23
4.2 TIME DELAY	25
4.3 MATCHING	26
5 RESULTS	28
5.1 TRANSMISSION COEFFICIENT	28
5.1.1 <i>Without 50 Ohm</i>	28
5.1.2 <i>With 50 Ohm</i>	30
5.2 REFLECTION COEFFICIENT	30
5.2.1 <i>Without 50 Ohm</i>	30
5.2.2 <i>With 50 Ohm</i>	32

5.3	FORWARD LOSS	32
5.3.1	<i>Without 50 Ohm</i>	32
5.3.2	<i>With 50 Ohm</i>	33
6	DISCUSSION.....	35
6.1	PRACTICAL ISSUES.....	35
6.1.1	<i>CST</i>	35
6.1.2	<i>Standing wave</i>	35
6.2	REFLECTION COEFFICIENT	35
6.2.1	<i>Wire</i>	35
6.2.2	<i>Impedance matching</i>	35
6.3	STABILITY.....	36
6.4	TRANSFER RATE VS ANTENNA TYPE	36
7	CONCLUSION	37
8	FURTHER WORK	38
8.1	CONNECTOR.....	38
8.2	ITERATIONS	38
	APPENDIX A.....	39
9	BIBLIOGRAPHY	41

List of Tables

TABLE 2-1 SHOWS THE PARAMETER VALUES FOR THE ORIGINAL ANTENNA USED BY WPC WITH REFERENCE TO THE DIMENSIONS SHOWN IN FIGURE 2-5.....	7
TABLE 2-2 SHOWS THE CALCULATED VALUES USING EQUATION (14) WITH AN B-VALUE OF 2.25MM, PERMITTIVITY OF SEAWATER WAS GIVEN IN [6] P.675 AND PERMITTIVITY OF POM IS GIVEN IN THE CST MATERIAL LIBRARIES.	15
TABLE 2-3 SHOWS THE VALUES USED FOR THE INITIAL SIMULATION AND THE VALUES USED IN THE PARAMETRIC STUDY SHOWN IN CHAPTER 3.2.2. THE VARIABLES ARE ILLUSTRATED IN FIGURE 2-8.....	15
TABLE 3-1 SHOW VARIABLES USED IN THE PARAMETRIC STUDY WITH ILLUSTRATION OF VARIABLES IN FIGURE 2-5	17
TABLE 3-2 SHOW VARIABLES FOR PARAMETRIC STUDY WITH ILLUSTRATION OF VARIABLES IN FIGURE 2-8	19
TABLE 3-3 LISTS SOME KEY NUMBERS FROM RESULTS SHOWN IN FIGURE 3-2.	21
TABLE 3-4 SHOW THE PARAMETERS USED FOR THE ORIGINAL DESIGN ANTENNAS. REFERENCE FOR VARIABLES ARE SHOWN IN FIGURE 2-5	21
TABLE 3-5 SHOW THE PARAMETERS USED FOR SELECTED OPEN COAX ANTENNAS. REFERENCE FOR VARIABLES ARE SHOWN IN FIGURE 2-8.....	22

List of Figures

FIGURE 1-1 SHOWS THE 150W-RSE SUBSEA CONNECTOR MALE AND FEMALE SIDE DISCONNECTED (A) AND CONNECTED (B). 1

FIGURE 2-1 (A) ILLUSTRATES THE DIFFERENT FIELDS AND BORDERS BETWEEN THEM FOR A GENERIC ANTENNA. FIGURE IS COPIED FROM FIGURE 2.7 IN [5]. (B) ILLUSTRATES THE PHASE DIFFERENCE IN RECEIVED SIGNAL FOR A GENERIC DIPOLE. 4

FIGURE 2-2 ILLUSTRATES A GENERIC 2-PORT SYSTEM OF S-PARAMETERS WITH THE ADDITION OF AN EXTRA PORT TO MODULATE LOST POWER IN EVENTUAL LOST HEATING OR RADIATION. 5

FIGURE 2-3 SHOWS THE ORIGINAL ANTENNAS USED BY WPC TODAY WITH TWO COAXIAL CABLES SOLDERED ON FOR MEASUREMENTS. ARROWS SHOW THE ANTENNAS USED FOR ETHERNET AND RS232/485 7

FIGURE 2-4 SHOWS THE REPRODUCTION OF THE ORIGINAL ANTENNA WHERE A) SHOWS THE CONNECTOR THAT FUNCTIONS AS A GROUND PLANE, AND B) SHOWS THE ANTENNA WITH THE CENTER CONDUCTOR. 8

FIGURE 2-5 ILLUSTRATES THE LAYOUT FOR THE NEW REPRODUCTION OF THE ORIGINAL ANTENNA EXPLAINED IN CHAPTER 2.3. (A) SHOWS THE TOP LAYER, WHERE THE CONNECTOR IT SOLDERED AS SEEN IN FIGURE 2-4 (A). AND (B) SHOWS THE BOTTOM LAYER WITH THE ANTENNA STRUCTURE AS SEEN IN FIGURE 2-4 (B)..... 8

FIGURE 2-6 ILLUSTRATES TWO DIFFERENT IMPLEMENTATIONS OF AN RF CONNECTOR IN ACCORDANCE WITH THE PRINCIPLES OF PATENT US5977841 A [13]. (A) SHOWS A CROSS SECTIONAL VIEW OF AN OPTIMAL DESIGN AND (B) SHOWS A CROSS SECTIONAL VIEW OF AN IMPLEMENTED DESIGN..... 10

FIGURE 2-7 ILLUSTRATES THE ELECTRIC FIELD IN A CROSS SECTION OF A SIMPLIFIED ANTENNA MODEL WHERE THE FIELD LINES ARE DRAWN SUCH THAT A THICK LINE INDICATES STRONG FIELD. THIS MODEL ILLUSTRATES HOW IT WOULD BE IF TWO COAXIAL CABLES ARE SET WITH THE OPENINGS AGAINST EACHOTHER..... 11

FIGURE 2-8 ILLUSTRATES THE TOP LAYER FOR THE ANTENNA WHERE RC IS THE RADIUS OF THE CENTER PLATE, RP IS THE RADIUS OUT TO THE SURROUNDING PLATES AND RG ARE THE RADIUS OF THE SURROUNDING GROUND PLATES. NOTE THAT THE SIZES ARE NOT COMPARABLE WITH ACTUAL DESIGN AND THAT THE NUMBER OF PLATES MAY WARY..... 11

FIGURE 2-9 ILLUSTRATES THE GROUND PLANE USED FOR THE ANTENNA WHERE THE HOLE IN THE CENTER IS TO HAVE SPACE TO THE CENTER CONDUCTOR OF THE MCX-CONNECTOR, AND THE CIRCULAR SHAPE IN THE CENTER IS TO SOLDER THE GROUND OF THE MCX-CONNECTOR. EACH OF THE FOUR PADS CONNECT TO THE FOUR PADS SEEN IN FIGURE 2-8..... 12

FIGURE 2-10 ILLUSTRATES THE CROSS SECTION OF AN COAXIAL CABLE WITH THE E-FIELD FROM AN **TEM11** WAVE PROPAGATING THROUGH THE CABLE, AND THE DIMENSIONS USED TO CALCULATE THE IMPEDANCE OF A COAXIAL CABLE..... 13

FIGURE 2-11 ILLUSTRATES HOW THE ANTENNAS ARE POSITIONED TO EACH OTHER AND WHICH MATERIALS ARE BETWEEN. THE LIGHT GREEN AREAS ARE THE PCB, THE LIGHT GREY ARE THE 2.5MM OF POM, AND THE LIGHT BLUE ARE THE 5MM OF SEAWATER. IT IS SHOWN THAT A VECTOR NETWORK ANALYZER WAS USED FOR MEASUREMENTS. 14

FIGURE 2-12 SHOWS THE SIMULATED VALUES OF S21 (A) AND S11 (B) 15

FIGURE 3-1 SHOWS THE TRANSMISSION COEFFICIENT FROM THE SIMULATIONS DONE BASED ON THE PARAMETERS IN TABLE 3-1..... 18

FIGURE 3-2 SHOWS RESULTS FROM SIMULATIONS OF THE OPEN COAXIAL ANTENNA AS DESCRIBED IN TABLE 3-2. (A), (B), (C) AND (D) SHOWS THE TRANSMISSION COEFFICIENT (S21) USING THE DIFFERENT PARAMETERS AND (E) SHOWS THE RELATIVE ROTATION LOSS AS EXPLAINED ABOVE. 20

FIGURE 3-3 SHOWS SIMULATED TRANSMISSION COEFFICIENTS (S_{21}) FROM THE CHOSEN ANTENNAS. (A) SHOWS S_{21} FOR THE *OPEN COAX ANTENNAS* DESCRIBED IN TABLE 3-4 AND (B) SHOWS S_{21} FOR THE *ORIGINAL DESIGN ANTENNAS* DESCRIBED IN TABLE 3-5 22

FIGURE 4-1 DESCRIBES THE MEASURING RIG USED. (A) SHOW THE RIG AND (B) ILLUSTRATES HOW THE RIG IS BUILT UP. THE TRANSMITTER PCB CAN BE MOVED TO INCREASE/DECREASE THE DISTANCE, D. SEALING RINGS ARE USED TO KEEP THE PCB'S DRY. 23

FIGURE 4-2 (A) SHOWS THE ORIGINAL ANTENNA WITH FERRITES. (B) SHOWS THE MEASUREMENT OF S_{21} WITH AND WITHOUT FERRITES AT A DISTANCE OF 5MM WATER. 24

FIGURE 4-3 SHOWS HOW THE MEASURED DELAY IS INSERTED USING THE TWO TIMEDELAY-BLOCKS. IT ALSO SHOWS HOW THE SNP1 IS USED TO LOAD THE DIFFERENT .S2P FILES FOR VIEWING..... 24

FIGURE 4-4 SHOWS THE LENGHT OF THE ADAPTER (LEFT) AND THE CONNECTOR WITH SHORT CIRCUITED(RIGHT)..... 25

FIGURE 4-5 SHOWS MEEASUREMENTS OF S_{11} ON THE VNA BEFORE (A) AND AFTER (B) TIME DELAY WERE ADJUSTED. 26

FIGURE 4-6 SHOWS S_{11} FOR A MEASUREMENT OF OPEN COAXIAL ANTENN CONFIGURATION A FROM 2GHZ TO 6GHZ WITH A 5MM SPACING BETWEEN THA PLASTIC. (A) WITHOUT CORRECTION ON TIME DELAY. (B) WITH CORRECTION ON TIME DELAY..... 26

FIGURE 4-7 SHOW EXAMPLES OF HOW THE RESISTORS ARE CONNECTED TO THE ANTENNAS. (A) SHOWS FOR *OPEN COAX ANTENNA* CONFIGURATION A. (B) SHOWS FOR *OPEN COAX ANTENNA* CONFIGURATION B..... 27

FIGURE 5-1 SHOWS THE TRANSMISSION COEFFICIENT (S_{21}) FOR THE *OPEN COAX ANTENNA* CONFIGURATION A TO C. (A) SHOWS THE MEASURED RESULT AND (B) SHOWS THE SIMULATED RESULTS..... 28

FIGURE 5-2 SHOWS THE TRANSMISSION COEFFICIENT (S_{21}) FOR THE *ORIGINAL DESIGN ANTENNA* CONFIGURATION A AND B. (A) SHOWS THE MEASURED RESULT AND (B) SHOWS THE SIMULATED RESULTS. 29

FIGURE 5-3 SHOWS A PLOT OF THE TRANSMISSION COEFFICIENT FOR THE *OPEN COAX ANTENNA* CONFIGURATION C WITH EXTENDED FREQUENCY RANGE FROM 2-10 GHZ AND THE DISTANCE 5MM..... 29

FIGURE 5-4 SHOWS A PLOT OF THE TRANSMISSION COEFFICIENT WITH A 50 OHM CONNECTED. (A) SHOWS FOR THE *OPEN COAX ANTENNAS* AND (B) SHOWS FOR THE *ORIGINAL DESIGN ANTENNAS*. 30

FIGURE 5-5 SHOWS THE REFLECTION COEFFICIENT (S_{11}) FOR THE *OPEN COAX ANTENNA* CONFIGURATION A TO C. (A) SHOWS THE MEASURED RESULT AND (B) SHOWS THE SIMULATED RESULTS..... 31

FIGURE 5-6 SHOWS THE REFLECTION COEFFICIENT (S_{11}) FOR THE *ORIGINAL DESIGN ANTENNA* CONFIGURATION A AND B. (A) SHOWS THE MEASURED RESULT AND (B) SHOWS THE SIMULATED RESULTS..... 31

FIGURE 5-7 SHOWS MEASUREMENTS OF REFLECTION COEFFICIENT IN A FREQUENCY SWEEP FROM 2 TO 6GHZ. (A) SHOWS MEASURMENTS ON THE *OPEN COAX ANTENNAS*, AND (B) SHOWS MEASUREMENTS ON THE *ORIGINAL DESIGN ANTENNAS*. 32

FIGURE 5-8 SHOWS THE FORWARD LOSS FACTOR DESCRIBED IN CHAPTER 2.1.4 FOR THE *OPEN COAX ANTENNA* CONFIGURATION A TO C. (A) SHOWS THE MEASURED RESULTS AND (B) SHOWS THE SIMULATED RESULTS. 33

FIGURE 5-9 SHOWS THE FORWARD LOSS FACTOR DESCRIBED IN CHAPTER 2.1.4 FOR THE *ORIGINAL DESIGN ANTENNA* CONFIGURATION A AND B. (A) SHOWS THE MEASURED RESULTS AND (B) SHOWS THE SIMULATED RESULTS. 33

FIGURE 5-10 SHOWS THE FORWARD LOASS FACTOR FOR THE MEASUREMENTS DONE WITH THE 50OHM RESISTOR CONNECTED TO THE ANTENNAS. (A) SHOWS FOR THE *OPEN COAX ANTENNAS* AND (B) SHOWS FOR THE *ORIGINAL DESIGN ANTENNAS*..... 34

FIGURE 34 SHOWS THE TRANSMISSION COEFFICENT FOR *ORIGINAL DESIGN ANTENNA* WITH CONFIGURATION A. (A) SHOWS WITH RESISTOR CONNECTED, AND (B) SHOWS WITHOUT ANY RESISTOR 39

FIGURE 6 SHOWS THE TRANSMISSION COEFFICIENT FOR *ORIGINAL DESIGN ANTENNA* WITH CONFIGURATION B. (A) SHOWS WITH RESISTOR CONNECTED, AND (B) SHOWS WITHOUT ANY RESISTOR.....39

FIGURE 14 SHOWS THE TRANSMISSION COEFFICIENT FOR *OPEN COAX ANTENNA* WITH CONFIGURATION A. (A) SHOWS WITH RESISTOR CONNECTED, AND (B) SHOWS WITHOUT ANY RESISTOR.....40

FIGURE 18 SHOWS THE TRANSMISSION COEFFICIENT FOR *OPEN COAX ANTENNA* WITH CONFIGURATION B. (A) SHOWS WITH RESISTOR CONNECTED, AND (B) SHOWS WITHOUT ANY RESISTOR.....40

FIGURE 10 SHOWS THE TRANSMISSION COEFFICIENT FOR *OPEN COAX ANTENNA* WITH CONFIGURATION C. (A) SHOWS WITH RESISTOR CONNECTED, AND (B) SHOWS WITHOUT ANY RESISTOR.....40

1 Introduction

In subsea, it is difficult to create connectors for power transfer or communication, therefore Wireless Power & Communication (WPC) have created a wireless connector shown in Figure 1-1. The incentive for this connector is that metals do not last long exposed to the salt water, and a closed waterproof connector is advantageous.

This master's thesis is a completion of the project written by the student [1] where the antenna used for data transfer in the connectors were analyzed. To analyze the antenna, measurements of s-parameters were done with two antennas pointing towards each other in a rig made to impersonate the connectors. The connector used is called 150W-RSE Subsea Connector found in [2].



Figure 1-1 Shows the 150W-RSE subsea connector male and female side disconnected (a) and connected (b).

1.1 Motivation and goals

The connector from WPC found in [2] have three ways of transfer, first is the power transfer on 150W done in the 100KHz frequencies, this is done using coiled wires like an AC transformer with a set relation. Second is an RS232/485 link with 115kbps transfer rate, this is done using an inductive link on the edges of the PCB seen in Figure 2-3 with a frequency on the 10-30MHz band. The last link is the one this master's thesis is focused on, where today's solution is shown in Figure 2-3.

The transfer rate of the connector is listed as 15Mbps [2]. The system uses a chip called WizFi630 which has a receive sensitivity on -66dBm using a bandwidth of 40MHz and an output power of 14dBm. The frequency range for Europe is 2.4-2.483 GHz, and therefore all calculations done are based on 2.4GHz. The goal for this master's thesis is to design a new antenna where the transfer rate is higher than 15Mbps. To achieve this, a reconstruction of the

original antenna were made and a parametric study was performed on this. In addition, a new antenna design is proposed with a similar parametric study. To be able to verify the simulations done, a measurement rig has been designed and built to mimic the environment in the connector. This measurement rig was used when measuring the s-parameters to ensure that the measurements can be repeated and get the same results.

2 Theory and literature research

2.1 Antenna parameters

Here the different parameters used to describe the antenna and antenna results are explained and some of the choices for measurements are done.

2.1.1 Electric length

When looking at a transmission line, the wave travels a certain distance (d) measured in meters [m], but for the different frequency, the phase is different on the output for the same length. Therefore, it is important to know the length of a line compared to the wavelength of the signal. To do this, equation (1) is used. [4]

$$L = \frac{d}{\lambda} = \frac{df\sqrt{\epsilon_r}}{c} \quad (1)$$

Here d , is the length of the transmission line in meters, λ is the wavelength of the signal in meters, ϵ_r is the permittivity of the material, f is the frequency of the signal in hertz and c is the speed of light in meters per second. L is the electric length which is unit less. The electric length is easy to interpret as an angle, where the full wavelength is 360 degrees. This way it is possible to talk about the electric length as degrees or phase.

$$\theta_L = L * 360 \quad (2)$$

When measuring a transmission line, the phase of S_{21} is equal to the phase length of the transmission line.

2.1.2 Near and far field

The fields surrounding the antenna is, according to [5] subdivided into three regions: The reactive near-field, the radiating near field and the far field. The division between these regions can be seen in Figure 2-1.

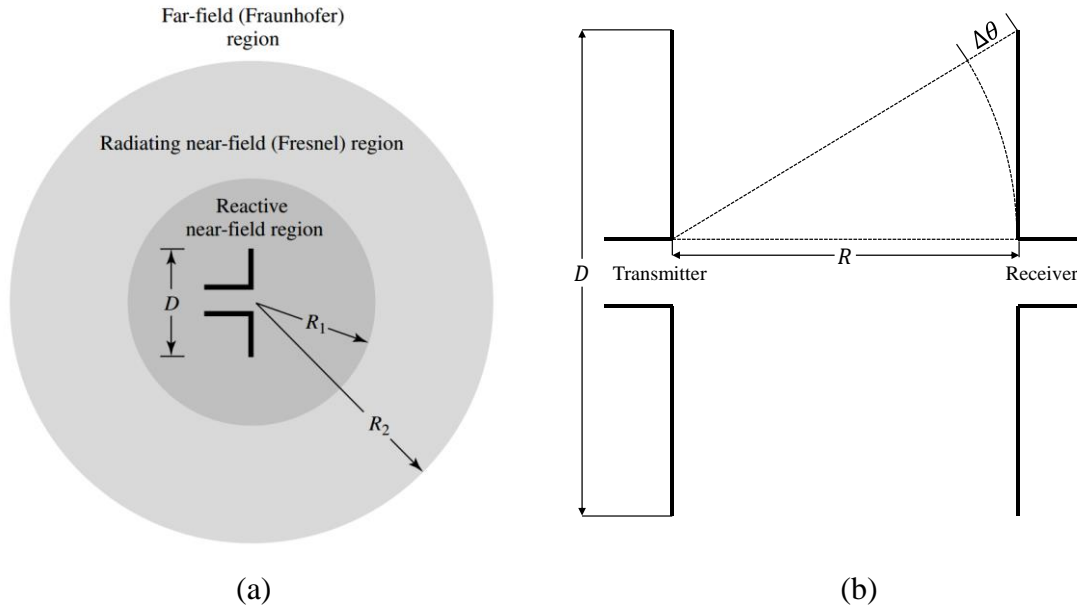


Figure 2-1 (a) illustrates the different fields and borders between them for a generic antenna. Figure is copied from figure 2.7 in [5]. (b) illustrates the phase difference in received signal for a generic dipole.

The reactive near-field region is dominated by reactive field components, and are located in the field immediately surrounding the antenna. The Far-field is where the reactive field components have diminished to negligible values and the radiation pattern does not change dependent on the distance. The equation for R_2 shown in equation (3) are derived from the fact that the phase difference ($\Delta\theta$) shall not exceed the length $\lambda \frac{22.5}{360}$ where $\Delta\theta$ are illustrated in Figure 2-1. According to [5] the boundaries R_1 and R_2 are given by the equations:

$$R_1 = 0.62\sqrt{D^3/\lambda} \quad (3)$$

$$R_2 = 2D^2/\lambda \quad (4)$$

In the equations above, λ is the wavelength in meters and D is the largest possible dimension on the antenna. When deriving the equations for R_1 and R_2 , some assumptions are made. These assumptions are that the distance, R , is much larger than the wavelength and much larger than the largest possible dimension of the antenna, D . The wavelength for this project is; $\lambda = c/f = 3 * 10^8 / 2.44 * 10^9 = 12.3cm$, the original antenna has a diameter (D) of 5.5mm. With a distance, R , of up to 10mm, it is clear that the mentioned assumptions can not be done and another solution to calculating the far field must be used. According to [6] the far-field of an antenna is given by:

$$2\pi R/\lambda \gg 1 \quad (5)$$

Where R is distance from antenna and λ is the wavelength of the antenna. If numbers are inserted, the value $2\pi R/\lambda = 0.05$ which is far below 1. Therefore the antennas are in the near field, which limits the options for measurements.

As mentioned, in the far-field, the radiation pattern does not change depending on distance, which makes it possible to measure the radiation pattern for a given distance, these measurements gives a gain in a certain direction, and transmitted effect is output effect, plus antenna gain for receiver and transmitter. In the near field, the radiation pattern may change depending on distance. Therefore, it is not viable to use the antenna chamber to characterize the antennas, but they should be placed in the position they are supposed to be used, and transmitted effect should be measured. The placement used is shown in Figure 2-11.

2.1.3 S-parameters

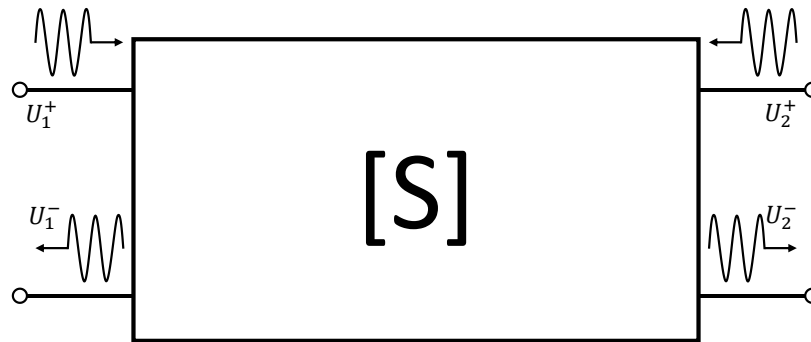


Figure 2-2 Illustrates a generic 2-port system of S-parameters with the addition of an extra port to modulate lost power in eventual lost heating or radiation.

When working with high frequency components, s-parameters may be used as a means for characterizing n-port networks, where n, is the number of connections in the network. One such network are illustrated in Figure 2-2 with two ports where each port have one incoming wave (+) and one outgoing wave (-). The s-parameters define the relationships between the different ports and are defined in equation (6).

$$\begin{bmatrix} U_1^- \\ U_2^- \end{bmatrix} = \begin{bmatrix} S_{11} & S_{12} \\ S_{21} & S_{22} \end{bmatrix} * \begin{bmatrix} U_1^+ \\ U_2^+ \end{bmatrix} \quad (6)$$

One of the benefits of using s-parameters is that they are relatively easy to measure. Equation (6) can be set up as two separate equations, and solved by short circuiting the different inputs and mathematically set either $U_1^+ = 0$ or $U_2^+ = 0$. Thus one can solve to find each s-parameter according to equation (6). [7]

$$S_{ij} = \frac{U_i^-}{U_j^+} \quad (7)$$

When using a vector network analyzer, the s-parameters contains both phase and amplitude, thus it is possible to see that for instance S_{11} contains what is returned to port 1 from port 1, and in which amplitude and phase. This can then be plotted in a smith chart to show impedance or visualize the reflected wave dependent of frequency.

2.1.4 Forward Loss Factor

In a passive system, some losses are expected. These losses can occur due to for instance resistive components, radiation and dielectric loss. To give an indication on how much of input power that dissipates in these losses, a loss factor is used. The loss factor described and used in [8] are divided in two separate factors. One Forward Loss Factor (FLF) and one Reflected Loss Factor (RLF) that are shown in equation (8) and (9) respectively.

$$FLF = 1 - |S_{11}|^2 - |S_{21}|^2 \quad (8)$$

$$RLF = 1 - |S_{22}|^2 - |S_{12}|^2 \quad (9)$$

The loss factors are described in [8] as the difference between a normalized input power and the power that is reflected and transmitted to the transmitter and receiver ports respectively.

It is important to note that this loss is different from mismatch loss ($1 - |S_{11}|^2$) since mismatch loss only shows how much power that is lost because of reflections.

2.2 Electrically short antennas

A definition of electrically short antennas is that the longest dimension of the antenna is no more than one-tenth of a wavelength. [9] This definition makes no distinction between different topologies but only the longest dimension of the antenna. Antennas for FM broadcast reception are sometimes reduced in size for convenience and portability. [9]

The 315 or 433 MHz wireless remote control and telemetry systems for keyless entry, garage door openers, wireless doorbells and remote-reading thermometers rarely have “full-size” resonant antennas, since a wavelength is around 1 meter. A $\lambda/4$ monopole would be 17 cm long, and requires a similarly sized ground layer. [9]

2.3 Original antennas

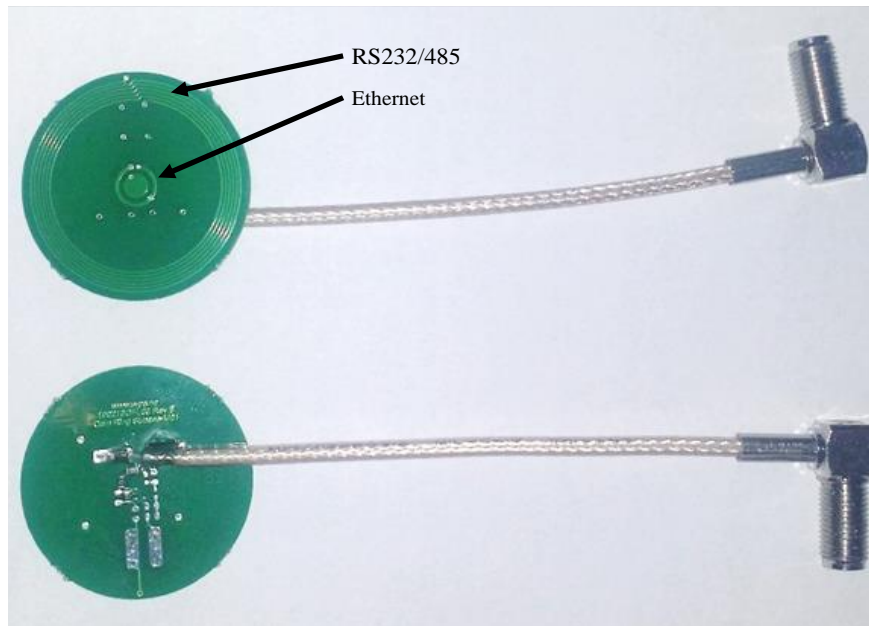


Figure 2-3 Shows the original antennas used by WPC today with two coaxial cables soldered on for measurements. Arrows show the antennas used for Ethernet and RS232/485

Table 2-1 shows the parameter values for the original antenna used by WPC with reference to the dimensions shown in Figure 2-5

Variable	Value [mm]
R1	1.6
R2	2.25
W	0.5

In this chapter, the original antenna design is revisited and an attempt to improve design is done. A new model is made in CST, where the PCB is simplified to include only the antenna itself and a coaxial MCX connector. The resulting PCB is shown in Figure 2-4 where the antenna itself is the same, but the connection is changed to use a MCX coaxial connector instead of the soldering used in the old antenna and shown in Figure 2-3. In addition an illustration of the new antenna model is shown in Figure 2-5. The reason for the simplification is to eliminate any

spurious effects given from having the different components and connections that are not used in this project.

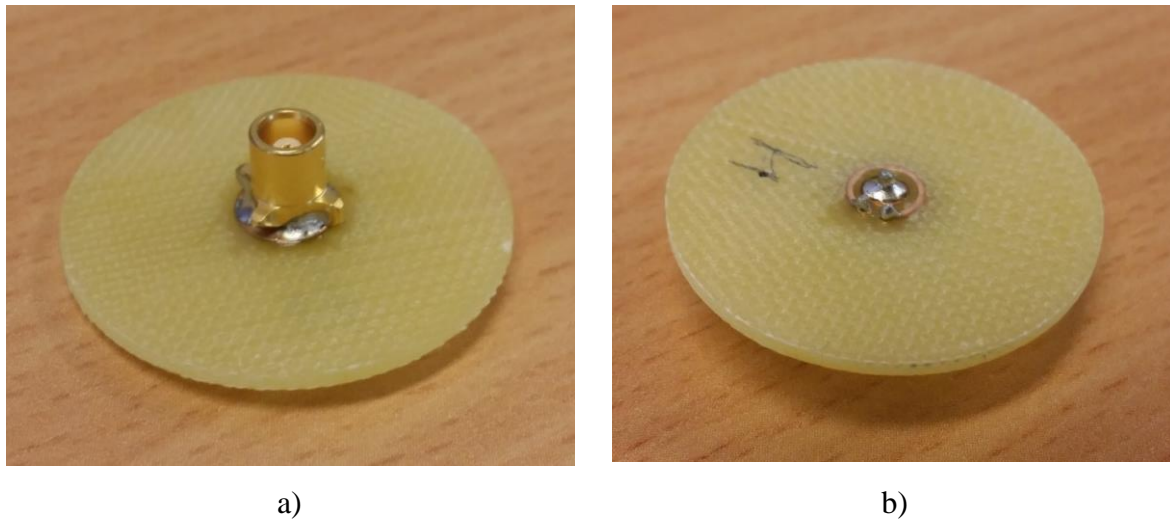


Figure 2-4 shows the reproduction of the original antenna where a) shows the connector that functions as a ground plane, and b) shows the antenna with the center conductor.

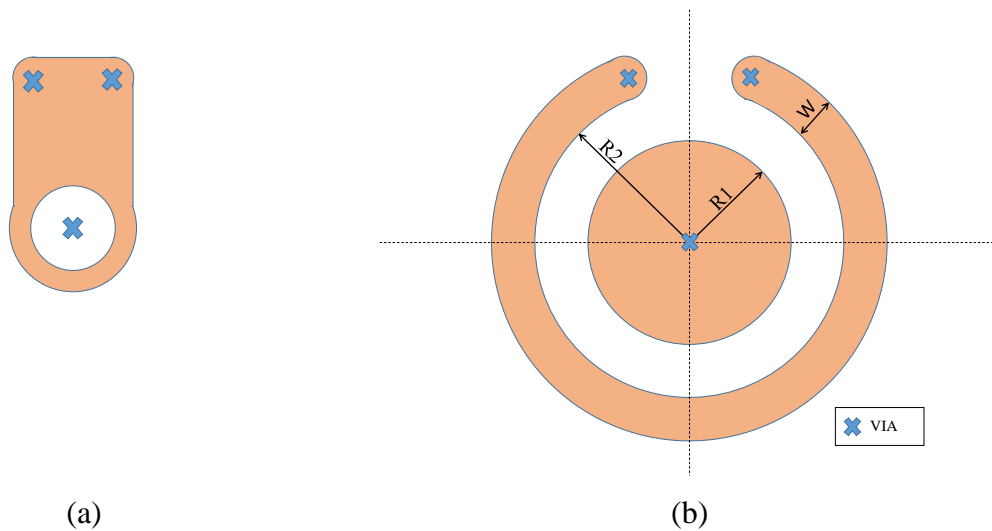


Figure 2-5 illustrates the layout for the new reproduction of the original antenna explained in chapter 2.3. (a) shows the top layer, where the connector it soldered as seen in Figure 2-4 (a). And (b) shows the bottom layer with the antenna structure as seen in Figure 2-4 (b)

To review the antenna design parameters shown in Figure 2-5 (b), a new parametric study is done and described in chapter 3.2.1.

2.4 New antennas

As a part of this project, some new antenna designs must be proposed and evaluated. To evaluate the new antennas, different design rules have been set using demands given from WPC or practical reasons:

- Fit the same PCB as the original antenna from WPC. (16mm in radius)
- No closed loops because of magnetic field from power transfer

2.4.1 Circular patch antenna

A circular patch antenna is chosen because of the simple structure and simplicity during simulations. Another reason is that the circular patch antenna radiates most normal to the PCB [10], and is therefore applicable to this project.

The circular antenna resonant frequency is given by the following equation [11]:

$$f^{(0)} = \frac{1.841}{2\pi a \sqrt{\epsilon\mu}} \quad (10)$$

Where a is radius of the disc in meter, $f^{(0)}$ is the frequency in GHz, ϵ is the relative permittivity of substrate and μ is the relative permeability of substrate. As mentioned in [12], equation (10) have an approximation error on 3 to 17%. Initial calculations show that with a frequency of 2.4GHz, and a FR4 substrate, the radius is calculated to be approximately 6.1cm. 6.1cm is a lot bigger than the radius of the circuit board (1.6cm). Even if accounting for an error on 17%, the smallest possible radius is as big as 5cm, which also is too large for this project.

In an attempt to decrease the area used, an increase in frequency is suggested. The wifi chip (WizFi630) does not support transmission in the 5GHz band, but WPC are interested in an eventual 5GHz design. With a frequency of 5GHz the radius is found to be approximately 2.6cm, which in the best case error of 17% may be 2.2cm. This radius is also larger than 1.6cm and the use of circular patch antennas are not discussed further in this project.

2.4.2 Open coaxial coupling antenna

The idea for this antenna was first discovered when reading patent US5977841 A [13], where the coaxial cable is tapered to give a wider radius on both the center conductor and the surrounding ground shield. The tapering described in the patent is shown in Figure 2-6 where

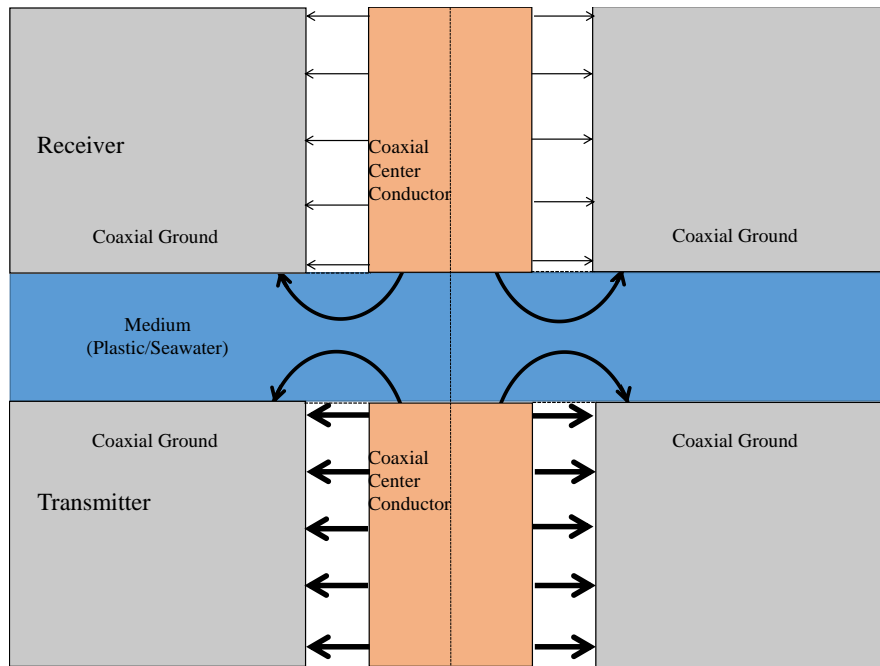


Figure 2-7 illustrates the electric field in a cross section of a simplified antenna model where the field lines are drawn such that a thick line indicates strong field. This model illustrates how it would be if two coaxial cables are set with the openings against each other.

Figure 2-7 illustrates how the electric field in an open coaxial coupling antenna would be, based on the TEM waves and initial evaluation of simulations done in CST. The illustration are drawn without any tapering or steps for simplicity.

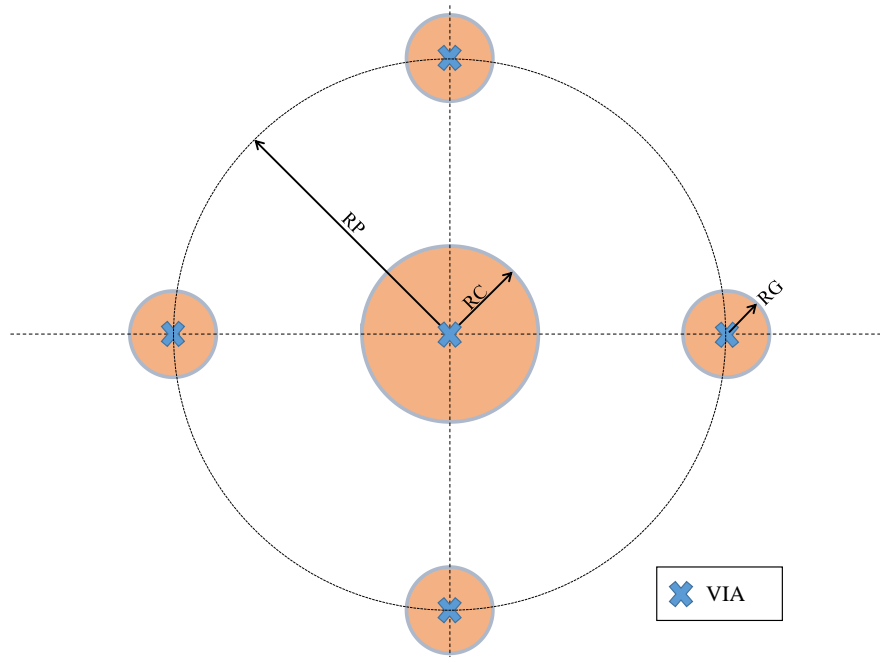


Figure 2-8 illustrates the top layer for the antenna where RC is the radius of the center plate, RP is the radius out to the surrounding plates and RG are the radius of the surrounding ground plates. Note that the sizes are not comparable with actual design and that the number of plates may vary.

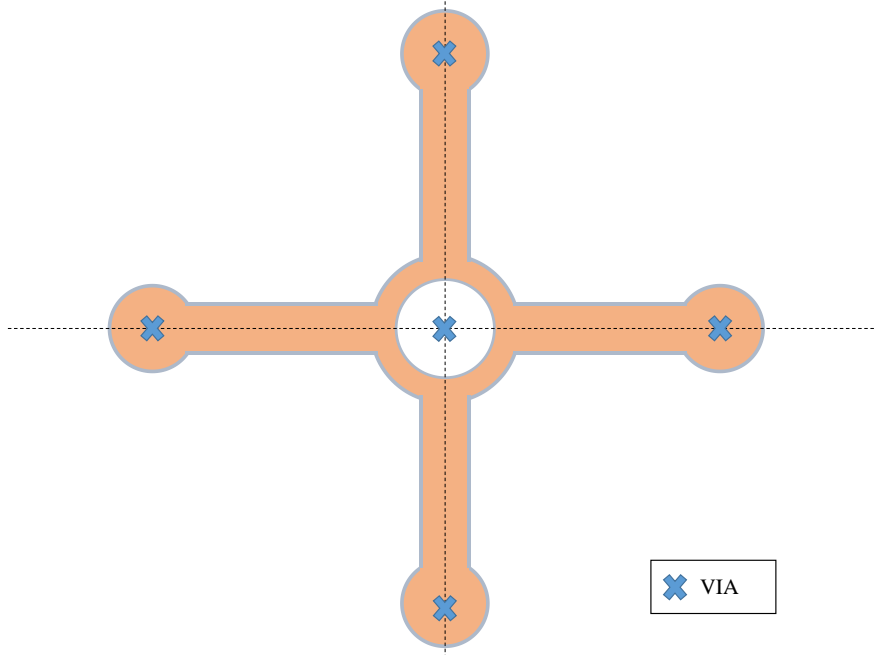


Figure 2-9 illustrates the ground plane used for the antenna where the hole in the center is to have space to the center conductor of the MCX-connector, and the circular shape in the center is to solder the ground of the MCX-connector. Each of the four pads connect to the four pads seen in Figure 2-8.

To decide the dimensions of the ground layer and center conductor, impedance matching has been chosen. According to [14], the impedance of a coaxial cable can be calculated by the following formula:

$$Z = \frac{1}{2\pi} \sqrt{\frac{\mu_r \mu_0}{\epsilon_r \epsilon_0}} \ln(b/a) = \frac{377}{2\pi} \sqrt{\frac{1}{\epsilon_r}} \ln(b/a) \quad (11)$$

Where μ is the permittivity of the material, ϵ is the permeability of the dielectric, a is the radius of the center conductor and b is the outer radius of the gap between the center conductor and outer conductor as illustrated in Figure 2-10. Since the substrate can be seen as isotropic and homogeneous with negligible magnetic properties, μ_r is set to one. As seen in (11), the impedance in a coaxial cable is only dependent of the relationship between a and b , and the value of ϵ_r . Since ϵ is dependent of the selected substrate, the only thing we can change is the size of a and b . The substrate used is FR4, which has a permeability of 4.7. By using this information, it is possible to change the sizes to match the impedance of the POM or seawater between the two connectors as shown in Figure 2-11. POM stands for Polyoxymethylene, and is an engineering thermoplastic with good electrical properties. According to the library in CST, the permittivity of POM is 3F/m.

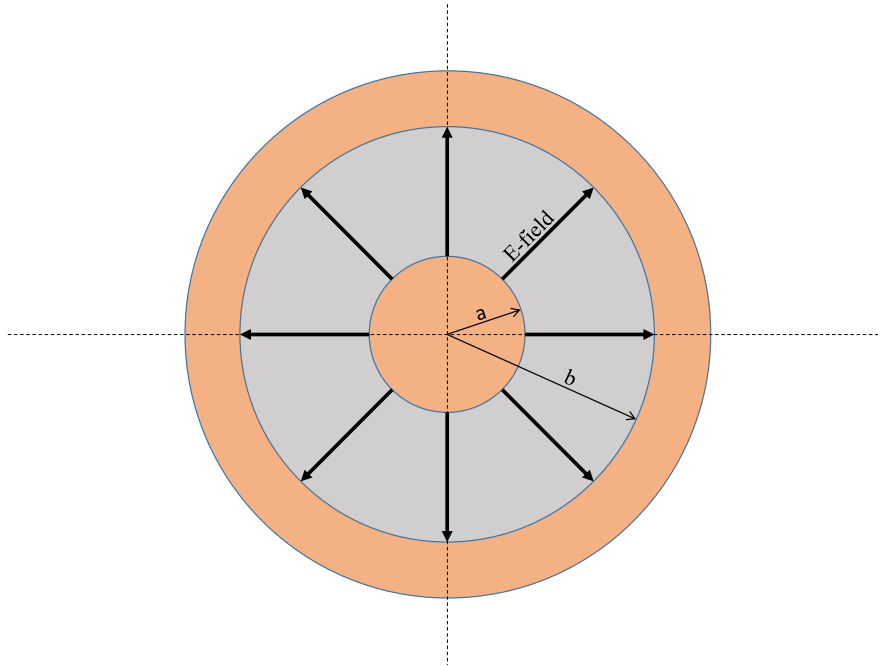


Figure 2-10 illustrates the cross section of an coaxial cable with the E-field from an TEM_{11} wave propagating through the cable, and the dimensions used to calculate the impedance of a coaxial cable.

In the first revision of the antenna, the total size is limited to the size of the original antenna. The reason for this is that the magnetic field from the power transfer is heating up the copper, and therefore the area should be as limited as possible. The value of b in (11) is set, while the value of a can vary to match the impedance. (11) is solved regarding to a :

$$a = b * e^{-\frac{Z2\pi\sqrt{\epsilon}}{377}} \quad (12)$$

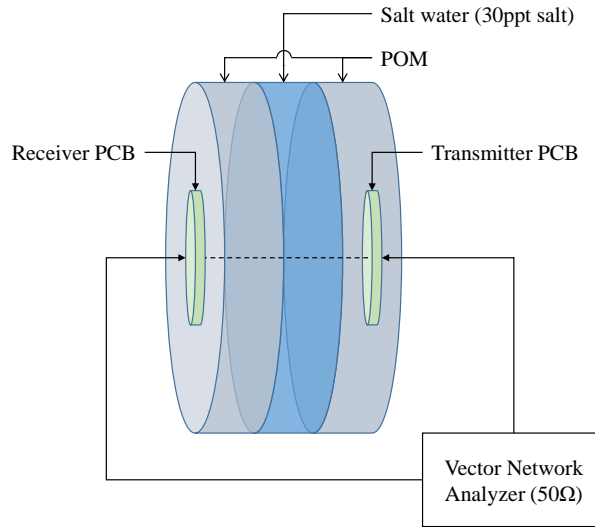


Figure 2-11 illustrates how the antennas are positioned to each other and which materials are between. The light green areas are the PCB, the light grey are the 2.5mm of POM, and the light blue are the 5mm of seawater. It is shown that a vector network analyzer was used for measurements.

Now that the impedance at the end of the antenna is known, the impedance of the materials between the antennas needs to be calculated. It is shown in [6] that the impedance in a material with given permittivity and permeability is given as:

$$Z = \sqrt{\frac{\mu_r \mu_0}{\epsilon_r \epsilon_0}} = 377 \sqrt{\frac{\mu_r}{\epsilon_r}} = \frac{377}{\sqrt{\epsilon_r}} \quad (13)$$

Since the materials can be seen as isotropic and homogeneous with negligible magnetic properties, the relative permeability is set to one. Therefore the impedance is only dependent on the permittivity of the materials. Now equation (13) is inserted to equation (12), and it is important to note, that the two ϵ_r is for the two different materials. In (12) ϵ_r is for the PCB substrate and in (13) it is for the selected material. The resulting equation is:

$$a = b * e^{-2\pi \sqrt{\left(\frac{\epsilon_{substrate}}{\epsilon_{material}}\right)}} \quad (14)$$

In equation (14) it should be noted that the value of a may never be greater than the value of b, since the exponent always is negative. To decide a value for the inner radius of the ground circle, the old design is used as a limiter of area to use. Since the existing design works, the

current design should be limited to this size. The ground circle on the old design had an outer radius of 2.75mm and an inner radius of 2.25mm.

Table 2-2 shows the calculated values using equation (14) with an b-value of 2.25mm, permittivity of seawater was given in [6] p.675 and permittivity of POM is given in the CST material libraries.

Material	Permittivity [F/m]	Impedance [Ω]	a [mm]
POM	3	218	0.001
Seawater	72	44.43	0.57

As seen in Table 2-2, the desired radius to match for the plastic covering the antenna is extremely small for a pcb-design, therefore the initial design of the new antenna will be simulated with a radius of 0.6mm.

Table 2-3 Shows the values used for the initial simulation and the values used in the parametric study shown in chapter 3.2.2. The variables are illustrated in Figure 2-8

Variable	Initial Value [mm]	Value for parametric study [mm]
RC	0.6	1.6
RP	2.75	4
RG	0.5	0.7

The results from this simulation is shown in Figure 2-12, .and it can be seen that the best transmission is on 6GHz, where $S_{21_{dB}}$ is -47.2dB.

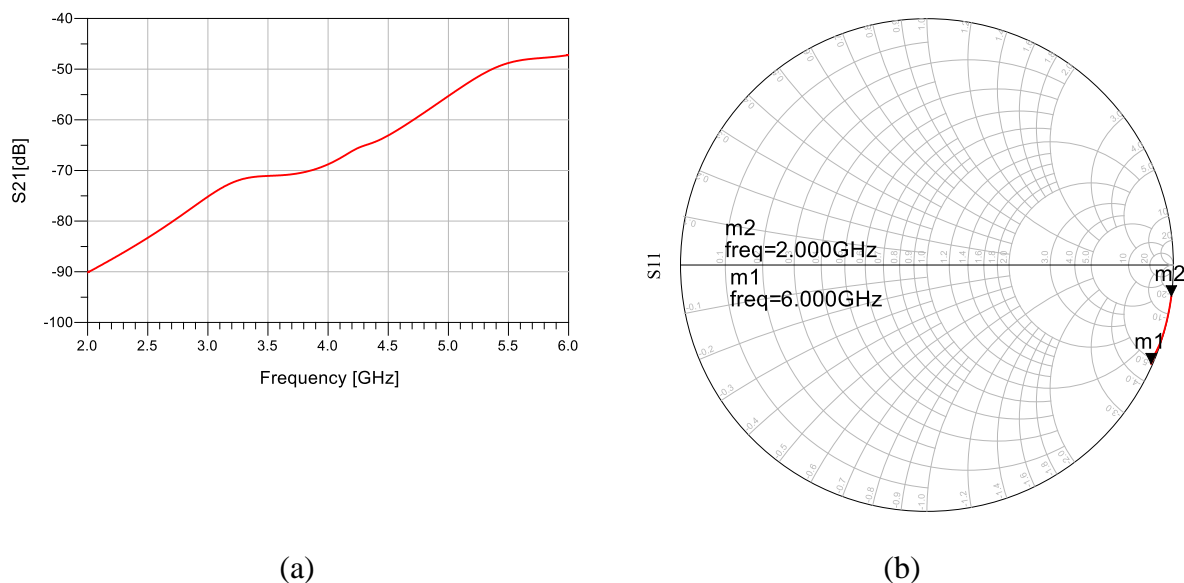


Figure 2-12 Shows the simulated values for the initial values listed in Table 2-3 (a) shows S_{21} , and (b) shows S_{11}

The transmission at the wanted frequency (2.4GHz) is as low as -84.8dB. As mentioned in chapter 1.1, the lowest possible transmission is as low as $-66\text{dBm}-14\text{dBm}=-80\text{dB}$, this gives a leeway of 4.8dB, which is too little. Therefore, a parametric study is performed to find a more satisfying configuration. To perform this parametric study, a set of parameters presented in Table 2-3 are used as a basic configuration. These parameters are chosen based on the fact that the via to the ground plates must be soldered, and some pads are needed, and the center is chosen to be the same as the original antenna from WPC. The parametric study can be seen in chapter 3.2.2.

3 Models in CST

3.1 Expanded model

The model has been improved to include a model of the connector house, which has been done by adding a layer of POM between the antennas, and a cylinder surrounding the PCB to mimic the measurements model seen in figure Figure 4-1 .

3.2 Parametric study

A parametric study is done by changing one of the parameters and observing the resulting S-parameters and evaluate what the different changes in variables does for the transmission coefficient. The optimal result is to adjust for better transmission trough the antennas. The goals will be as mentioned in chapter 1.1, that the transmission coefficient is highest at 2.4GHz, but it is also acceptable if 5GHz is chosen instead.

3.2.1 Original design antennas

When performing the parametric study, the variables in Table 3-1 are simulated from the min to the max value. In Table 3-1, the variable RC is the radius of the center patch of the antenna, RP are the radius out to the center of the ground plates and RG is the radius of these ground plates. The resulting transmission coefficients are plotted in the selected graphs in Figure 3-1.

Table 3-1 show variables used in the parametric study with illustration of variables in Figure 2-5

Variable	Min [mm]	Max [mm]	Results in Figure 3-1
R1	1.5	1.7	(a)
R2	2	2.5	(b)
W	0.4	0.6	(c)

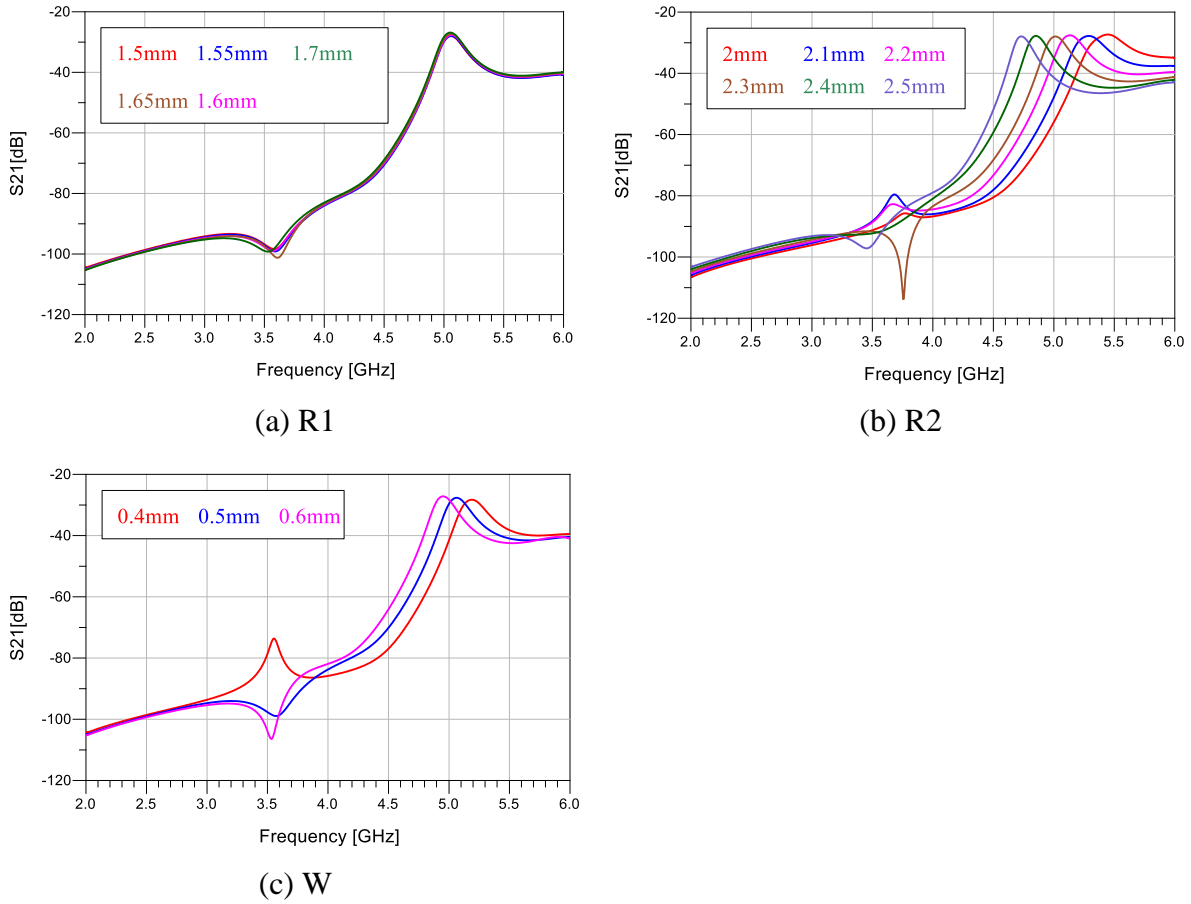


Figure 3-1 Shows the transmission coefficient from the simulations done based on the parameters in Table 3-1.

As seen in Figure 3-1 (a), changing the radius of the center patch of the antenna (R1) does not change much in the transmission. It can be seen in Figure 3-1 (b) that by changing the radius to the ground circle (R2) it is possible to change the frequency of the peak, this peak is moved linearly dependent on the value of R2. To find a formula for this peak, two known points are needed, for this calculation the peak when R2 is 2 and 2.5mm are used, where the peak are at 5.45 and 4.73GHz respectively. The following equation is created:

$$f_{peak} = x - yR2 \quad (15)$$

Where x is the value of f_{peak} when R2 is 0, and y is the gradient. With values inserted, the equation becomes:

$$f_{peak} = 8.33 - 1.44R2 \quad (16)$$

Where f_{peak} is given in GHz and R2 is given in mm. By using this equation, it is possible to adjust the peak frequency of the antenna by adjusting the radius to the ground circle. A similar

effect is seen in Figure 3-1(c), where the peak gets lower in frequency if the width of the ground circle increases. Using the same procedure as with equation (19) and using the values for the width (W) is 0.4 and 0.6mm with the frequencies 5.19 and 4.95GHz respectively we get:

$$f_{peak} = 5.64 - 1.15W \quad (17)$$

Where f_{peak} is given in GHz and W is given in mm. By using this equation, it is possible to adjust the peak frequency of the antenna by adjusting the width of the ground circle.

3.2.2 Open coaxial antennas

When performing the parametric study, the variables in Table 3-2 are simulated from the min to the max value. In Table 3-2, the variable RC is the radius of the center patch of the antenna, RP are the radius out to the center of the ground plates and RG is the radius of these ground plates. The results are shown in the selected plot in Figure 3-2.

Table 3-2 show variables for parametric study with illustration of variables in Figure 2-8

Variable	Min [mm]	Max [mm]	Results in Figure 3-2
RC	1.5	1.7	(a)
RP	3	6	(b)
RG	0.6	0.8	(c)
Number of Pads	4	9	(d) and (e)

When choosing the number of pads, the transmission coefficient will be evaluated, but another important feature is how well the antenna handles rotation. By request from WPC, the transmission factor should not change drastically when rotating the antenna. To evaluate this, a new variable is created called Relative Rotation Loss that is given in dB. The Relative Rotation Loss is just how many decibel one would lose if one of the antennas rotate θ_{error} degrees compared to the other antenna. The value θ_{error} is dependent on the number of pads on the antenna and is given by the formula:

$$\theta_{error} = \frac{180}{\text{Number of pads}} \quad (18)$$

To measure Relative Rotation Loss, one simulation is done without any rotation ($S_{21}(0^\circ)$) and one simulation is done with a rotation of θ_{error} ($S_{21}(\theta_{error})$). Then the Relative Rotation Loss is calculating using the following equation:

$$RRL_{dB} = S_{21}(0^\circ)_{dB} - S_{21}(\theta_{error})_{dB} \quad (19)$$

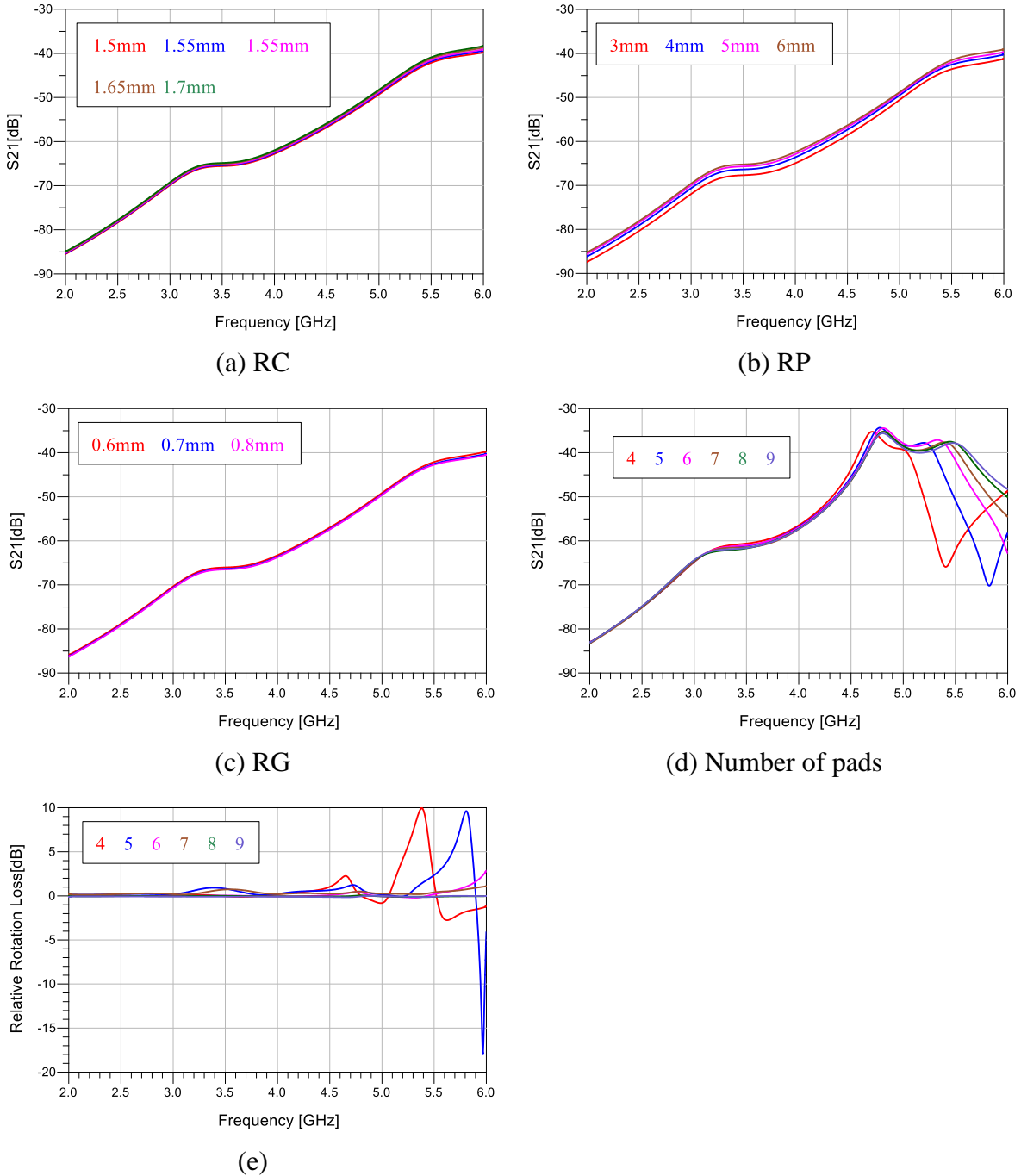


Figure 3-2 shows results from simulations of the open coaxial antenna as described in Table 3-2. (a), (b), (c) and (d) shows the transmission coefficient (S_{21}) using the different parameters and (e) shows the Relative rotation loss as explained above.

As seen in Figure 3-2, the changes gives an increase in transmission, how much S21 increases in dB (ΔS_{21}) for the different variables are listed in Table 3-3. In Table 3-3, the variable RC is the radius of the center patch of the antenna, RP are the radius out to the center of the ground plates and RG is the radius of these ground plates.

Table 3-3 Lists some key numbers from results shown in Figure 3-2.

Variable	ΔS_{21} at 2.4GHz [dB]	ΔS_{21} at 6GHz [dB]
RC	0.6	1.46
RP	2.3	2.2
RG	0.4	0.8

Table 3-3 shows that the biggest change is when changing the value RP, which also is the value with the biggest possibility for change if using the whole board is possible. By running several simulations, it could be seen that a peak in the transmission coefficient where placed in a frequency above 6GHz, and by increasing the value of RP, this peak where moved lower in frequency. With an RP=13.8, this peak is placed at 4.8GHz as seen in Figure 3-3. To place the peak at 2.4GHz, a larger PCB is needed. The peak is placed below 5GHz to give a flatter response at 5GHz.

As seen in Table 3-5, two additional antennas where made with this design, one were chosen to observe how good it would perform compared to the original antenna if given approximately the same size. The last antenna where made to see if the behavior seen in Figure 3-2 (a) is correct.

3.2.3 Chosen antenna designs

Five antennas were chosen to print on a PCB and measure on. Two of these antennas will be referenced to as *original design antenna configuration A/B*, where the different configurations are listed in Table 3-4. In Table 3-4, the variable R1 are the radius of the center patch of the antenna, R2 are the radius out to the ground circle and W is the width of this ground circle.

Table 3-4 show the parameters used for the *original design antennas*. Reference for variables are shown in Figure 2-5

Variable	Configuration	A	B
	R1	1.6	1.6
	R2	2.25	11
	W	0.5	0.5

Three of these antennas will be referenced to as *Open coax antenna A/B/C*, where the different configurations are listed in Table 3-5. In Table 3-5, the variable RC is the radius of the center patch of the antenna, RP are the radius out to the center of the ground plates and RG is the radius of these ground plates.

Table 3-5 show the parameters used for selected *open coax antennas*. Reference for variables are shown in Figure 2-8

Variable	Configuration	A	B	C
RC		2	1.6	1.6
RP		4	4	13.8
RG		0.7	0.7	0.7

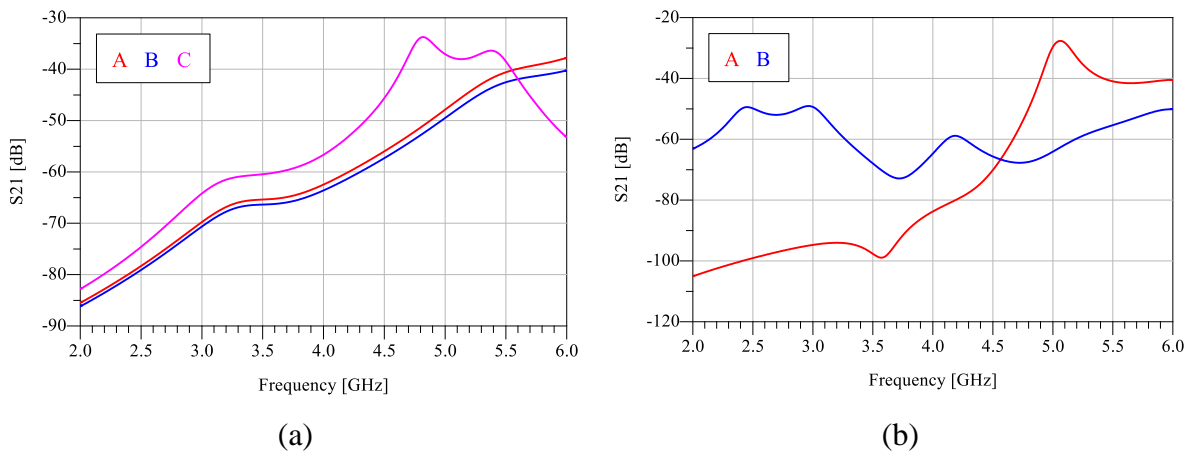


Figure 3-3 Shows simulated transmission coefficients (S21) from the chosen antennas. (a) Shows S21 for the *open coax antennas* described in Table 3-4 and (b) shows S21 for the *original design antennas* described in Table 3-5

4 Measurements

4.1 Measurement techniques

All measurements of S-parameters were done using a Vector Network Analyzer (VNA) in microwave lab here at NTNU. This VNA has been calibrated using SOLT which measures 4 known components (Short, Open, Load and Thorough) and then uses the measurements to remove errors in the equipment. To further improve the measurements, a test bench was built as illustrated in Figure 2-11 and shown in Figure 4-1 to mimic the connector and water in between. The water used in measurements were tap water mixed with 35ppt table salt to create seawater [15]. All measurementns are done with $D=5\text{mm}$. Measurements of the transmission coefficient with other values of D is given in Appendix A, and will not be discussed in this thesis.

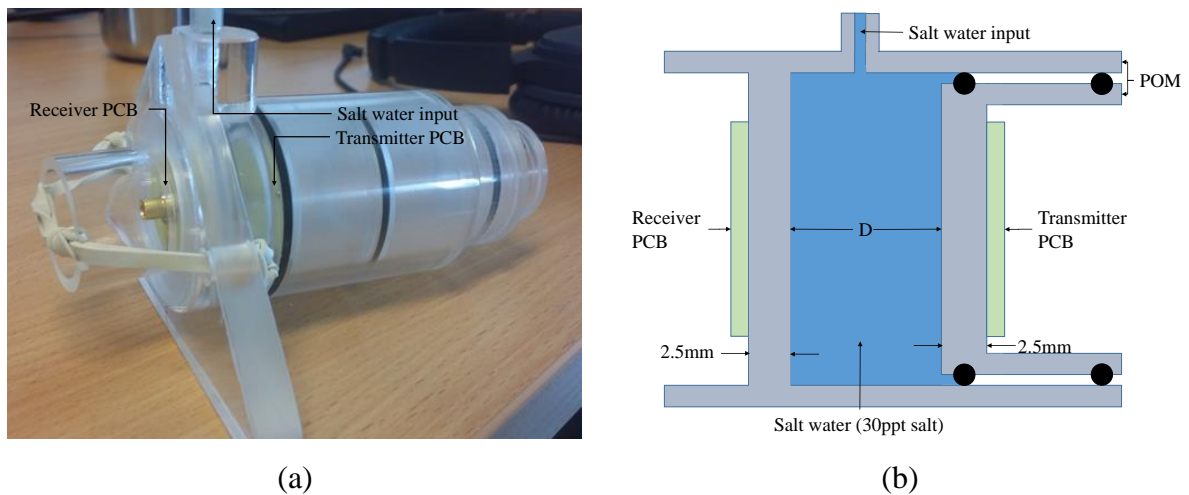
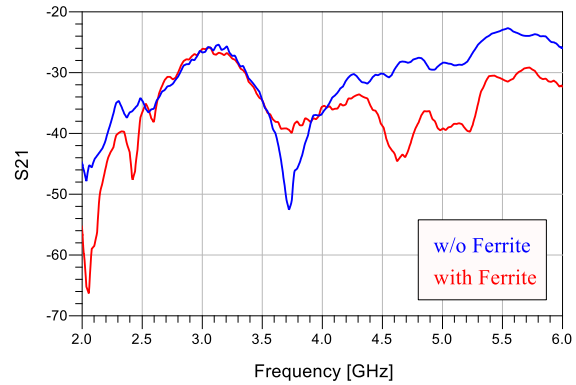


Figure 4-1 describes the measuring rig used. (a) Show the rig and (b) illustrates how the rig is built up. The transmitter PCB can be moved to increase/decrease the distance, D . Sealing rings are used to keep the PCB's dry.

During the project [1], WPC mentioned that the measurements on the antenna were unstable and that this could be noticed by stroking the coaxial cable connecting the antenna. If the transmission coefficient varies depending on where and how you touch the coaxial cable, the reflected currents interferes too much with the transmission. Therefore, ferrites were mounted on the coaxial cable connecting to the antenna as shown in Figure 4-2 (a). The reason for this is to create a resistance to the reflecting currents on the coax. During measurements, the S_{21} continued to be highly dependent on physical contact on the coaxial cable.



(a)



(b)

Figure 4-2 (a) Shows the original antenna with ferrites. (b) shows the measurement of S21 with and without ferrites at a distance of 5mm water.

All measurements are done with a VNA, thus all measurements are given in a touchstone (.s2p) format. And all simulations done in CST have been exported in a touchstone format. To plot and compare these results, Advanced Design System (ADS) were used, where a schematic as seen in Figure 4-3 were used to import the files and plot the different parameters in the data display window. All calculations were done locally in ADS using equations.

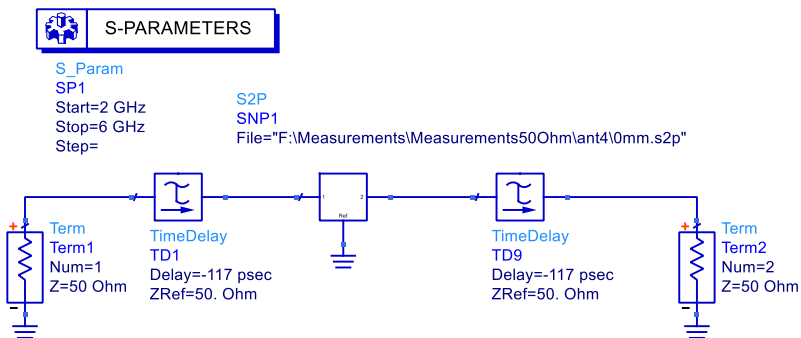


Figure 4-3 Shows how the measured delay is inserted using the two TimeDelay-blocks. It also shows how the SNP1 is used to load the different .s2p files for viewing.

4.2 Time delay

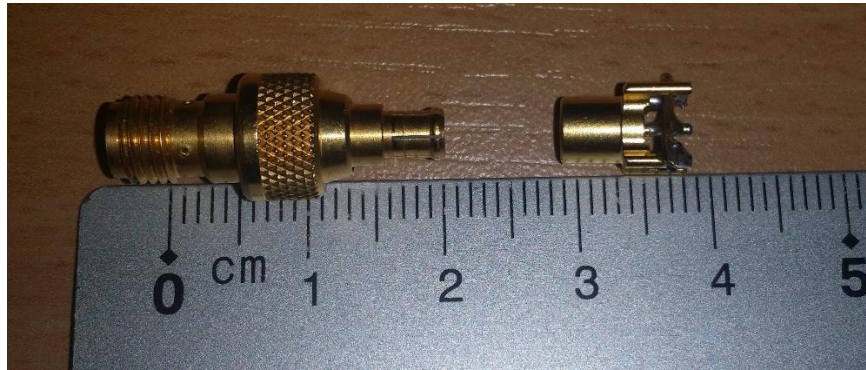


Figure 4-4 shows the length of the adapter (left) and the connector with short circuited(right)

The antenna uses MCX-connectors, and the VNA at the lab uses SMA-connectors which results in the use of an adapter as seen in Figure 4-4. When doing measurements on high frequency components, the VNA must be calibrated using SOLT. SOLT uses known components for Short, Open, Load and Through on each port and therefore calibrating away any errors in the LNA. The SOLT calibration is done on the SMA port of the LNA, therefore the length of the adapter and connector shown in Figure 4-6, will add a set physical length on the measurements that can be calculated to a phase using equation (2) given in 2.1.1. In this equation, both the distance, d , and speed of light, c , are constants, but as the frequency increases, the phase increases linearly. Therefore, one will get the rotating value of S_{11} as seen in Figure 4-6.

To counter the rotation of S_{11} , it is possible to insert a negative delay in ADS as shown in Figure 4-3, but to find the correct time delay to insert, measurements had to be done. There's two different ways to solve this problem, one is to measure the added length from the adapter, and calculate the delay using equation (20), where τ is the calculated delay, d , is the distance and c is the speed of light. Using this equation and measurements seen in Figure 4-4, the time delay is calculated to be $\tau = 2.8cm/c = 9.33 * 10^{-11}sec = 93.3psec$.

$$\tau = \frac{d}{c} \quad (20)$$

The second way to find the time delay is by measurements. To measure the time delay, a connector is short-circuited as seen in Figure 4-4, and then it is connected to the VNA through the adapter. In the VNA, it is possible to adjust the negative electric delay while observing the measurements. Since the port is short-circuited, S_{11} should be at 180 degrees, but because of the new length, it was drawn around the smith-chart. Then the negative delay where adjusted

until the results converge to 180 degrees. The difference in measurements are shown in Figure 4-5. The measured time delay was found to be 117 psec, which is not far from the calculated value of 93.3 psec.

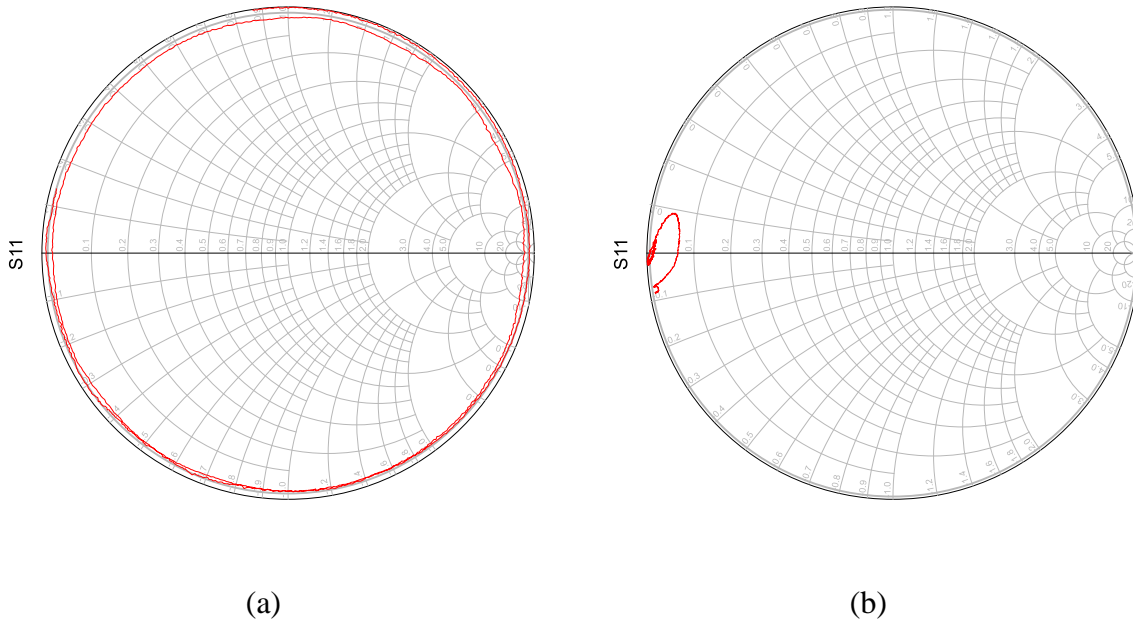


Figure 4-5 Shows measurements of S_{11} on the VNA before (a) and after (b) time delay were adjusted.

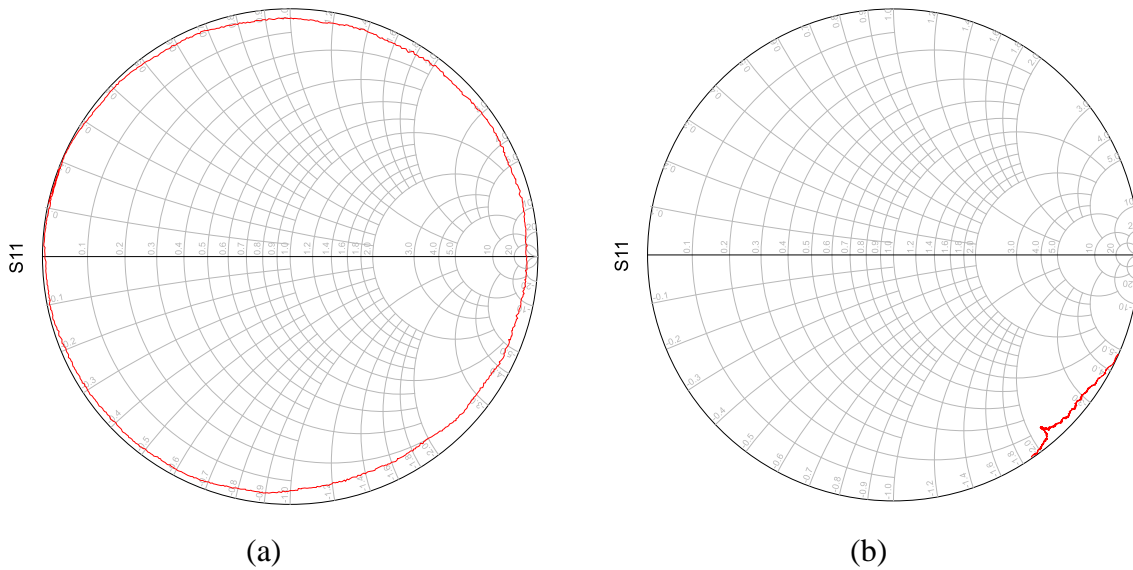


Figure 4-6 Shows S_{11} for a measurement of Open coaxial antenna configuration A from 2GHz to 6GHz with a 5mm spacing between the plastic. (a) without correction on time delay. (b) With correction on time delay.

4.3 Matching

When doing measurements on the antennas, it became apparent that the measurements were unstable. By touching the coaxial cable connecting the antenna, the transmission coefficient

would change up to 10dB. When observing the reflection coefficient, it was observed that the absolute value of S_{11} was close to 1, meaning that most of the wave is reflected, and that it is in the high impedance section of the smith-chart. These measurements can be seen in chapter 5.2.1. WPC suggested that inserting a 50 Ohm resistor between the center patch of the antenna and ground, it would decrease the instability. A 0805 SMA resistor of 56 Ohm is used on the antennas and are soldered as seen in Figure 4-7.

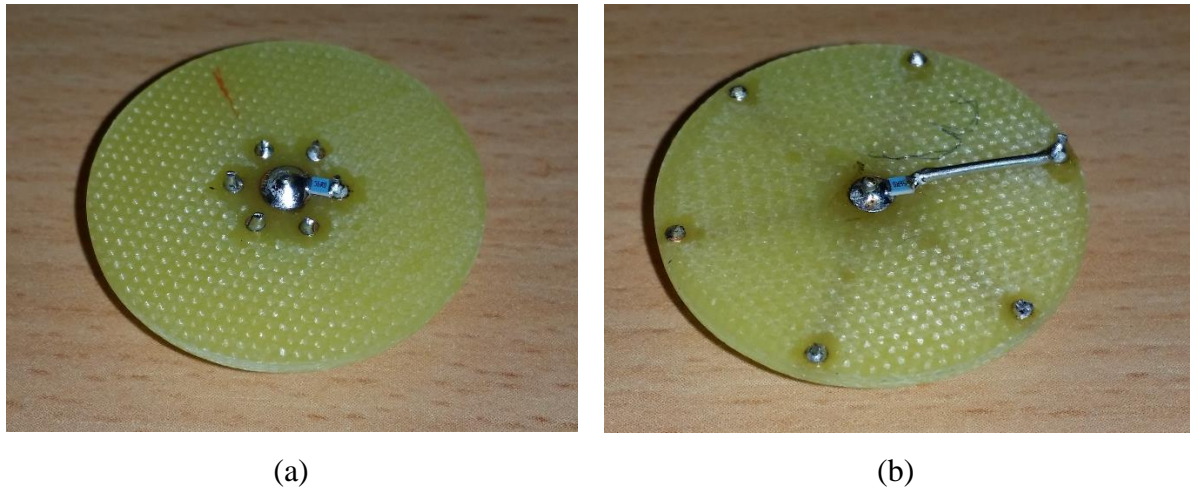


Figure 4-7 show examples of how the resistors are connected to the antennas. (a) shows for *Open coax antenna configuration A*. (b) shows for *Open coax antenna configuration B*.

As seen in Figure 4-7 (b), to connect the resistor, a piece of wire had to be used, this will create some inductive effects in addition to the resistance. Since the idea to add a resistor to the antennas were introduced late in the project, there was not enough time to include simulations of the new antennas. The measurements done are shown in separate sections in chapter 5.

5 Results

All of the printed antennas described in chapter 3.2.3 are set in the measurement rig described in chapter 4.1, and a sweep from 2-6GHz is done. Some of the measurements are done with a 56 Ohm resistor soldered between ground and center conductor as discussed in chapter 4.3. These results are listed in subsections called “with matching”, and measurements done without the resistor are placed in subsections called “without matching”.

5.1 Transmission coefficient

5.1.1 Without 50 Ohm

The transmission coefficient where measured for each of the five antennas with no resistor connected. S_{21} for the *open coax antennas* are shown in Figure 5-1 (a) and S_{21} for the *original design antennas* are shown in Figure 5-2 (a). The transmission coefficient for the *open coax antenna* configuration C where also plotted in Figure 5-3 with an increased frequency range from 2-10GHz.

The transmission coefficient where also simulated for each of the five antennas with no resistor connected. Simulated S_{21} for the *open coax antennas* are shown in Figure 5-1 (b) and S_{21} for the *original design antennas* are shown in Figure 5-2 (b).

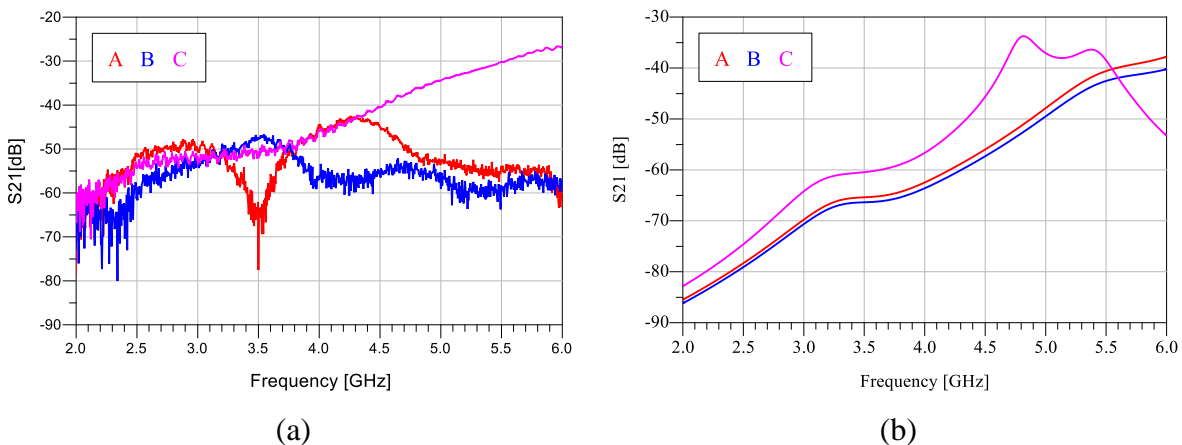
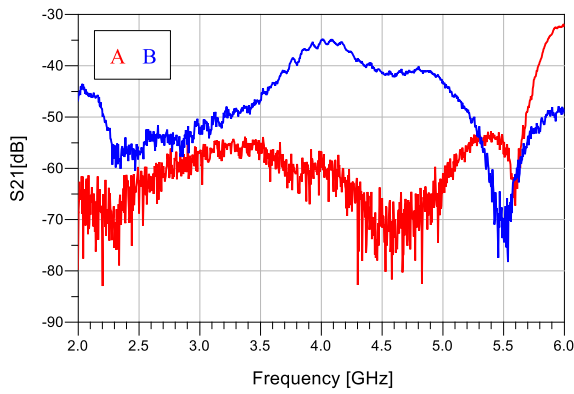
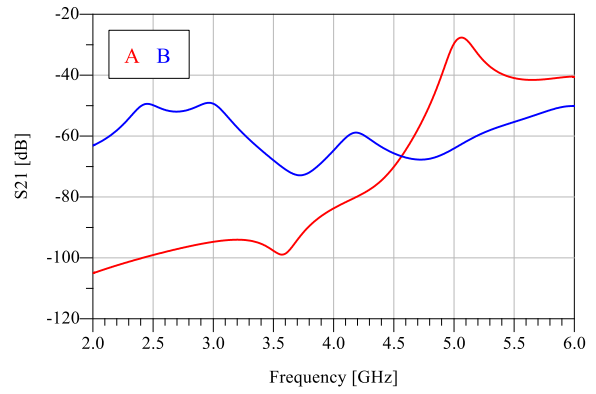


Figure 5-1 Shows the transmission coefficient (S_{21}) for the *Open coax antenna* configuration A to C. (a) shows the measured result and (b) shows the simulated results.

In Figure 5-1 it the values for configuration A and B are low as expected, and configuration C seems to be increasing even above 6GHz. Configuration A and B does not increase with the same rate in measurements as in simulations, but instead have a lower value through the entire sweep.



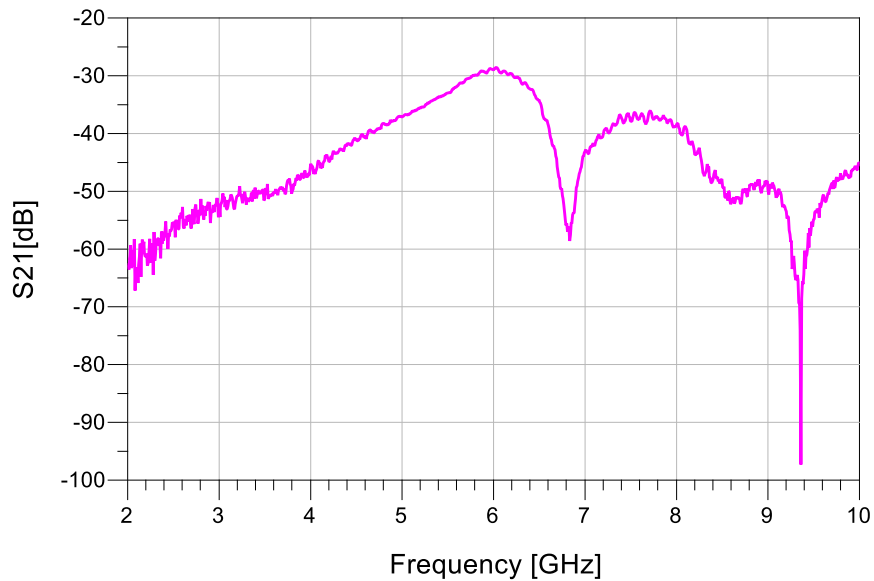
(a)



(b)

Figure 5-2 Shows the transmission coefficient (S_{21}) for the *Original design antenna configuration A and B*. (a) shows the measured result and (b) shows the simulated results.

As seen in Figure 5-2, both configurations have a frequency shift on 1 to 1.5GHz. The highest value for configuration B is measured to be -35.1dB, and the highest simulated value is -49.1dB. Configuration A have a measured maximum of -32.1dB with a highest simulated value of -27.7dB.



(a)

Figure 5-3 Shows a plot of the transmission coefficient for the *open coax antenna configuration C* with extended frequency range from 2-10 GHz and the distance 5mm.

As seen in Figure 5-3, the maximum for the transmission coefficient is at 6GHz and measures to be -28.6dB.

5.1.2 With 50 Ohm

The transmission coefficient where measured for each of the five antennas with the resistor connected. S_{21} for the *open coax antennas* are shown in Figure 5-4 (a) and S_{21} for the *original design antennas* are shown in Figure 5-4 (b).

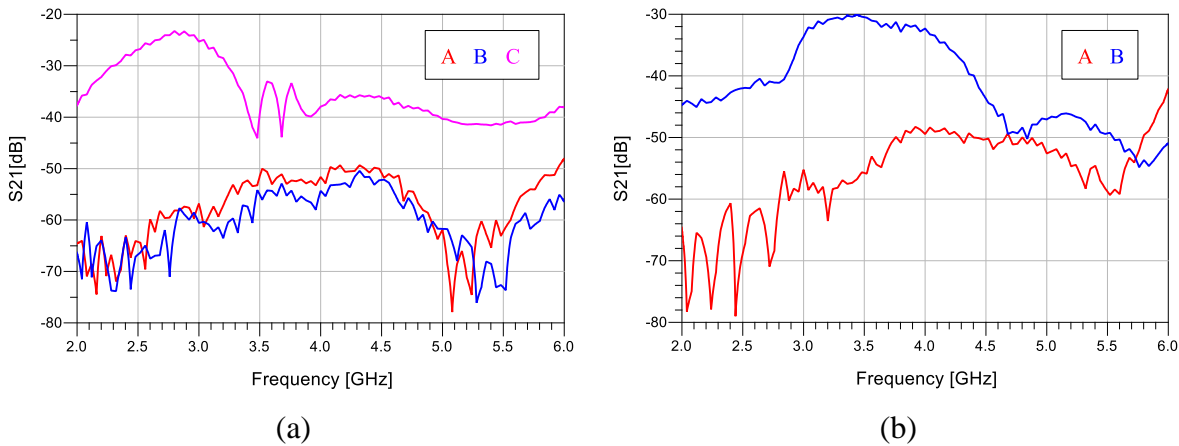


Figure 5-4 Shows a plot of the transmission coefficient with a 50 Ohm connected. (a) shows for the *open coax antennas* and (b) shows for the *original design antennas*.

As seen in Figure 5-4, the transmission coefficient of both the *open coax antennas* and the *original design antennas* are different compared to the results in section 5.1.1. The highest values for the *open coax antennas* are -48.1dB, -50.5dB and -23.3dB for configuration A,B and C respectively. The highest value for the *original design antennas* are -42.2dB and -30.1dB for configuration A and B respectively.

5.2 Reflection Coefficient

5.2.1 Without 50 Ohm

The reflection coefficient where measured for each of the five antennas without the resistor connected. The measured values of S_{11} for the *open coax antennas* are shown in Figure 5-5 (a), and S_{11} for the *original design antennas* are shown in Figure 5-6 (a).

The reflection coefficient were also simulated for each of the five antennas without the resistor connected. The simulated values of S_{11} for the *open coax antennas* are shown in Figure 5-5 (b), and S_{11} for the *original design antennas* are shown in Figure 5-6 (b).

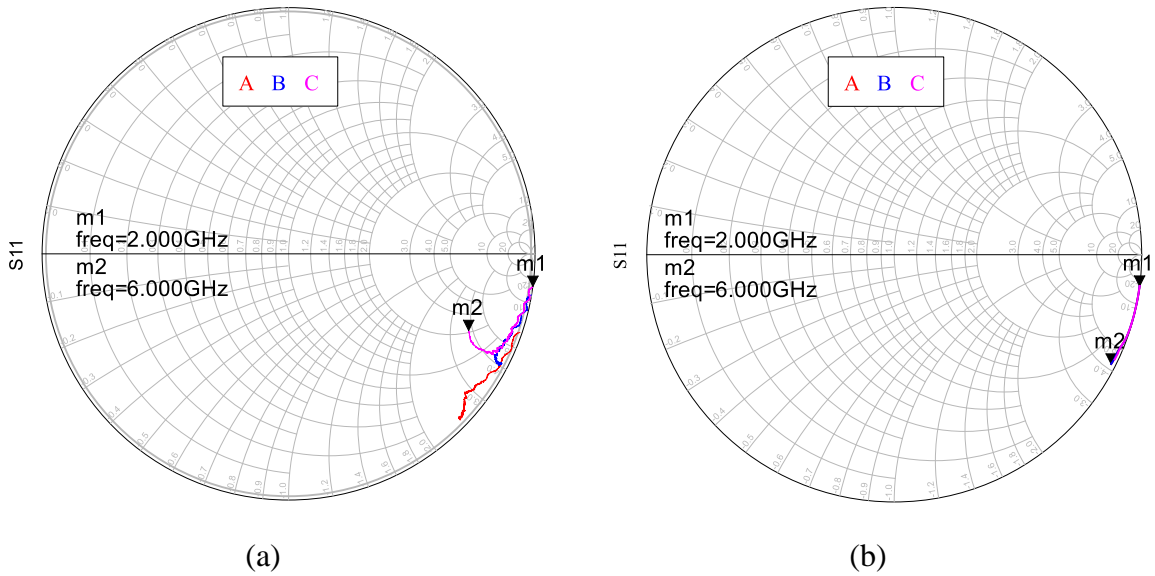


Figure 5-5 Shows the reflection coefficient (S11) for the *Open coax antenna* configuration A to C. (a) shows the measured result and (b) shows the simulated results.

As seen in Figure 5-5, the measured reflection coefficient for the *open coax antennas* in (a) are similar to the simulated ones shown in (b).

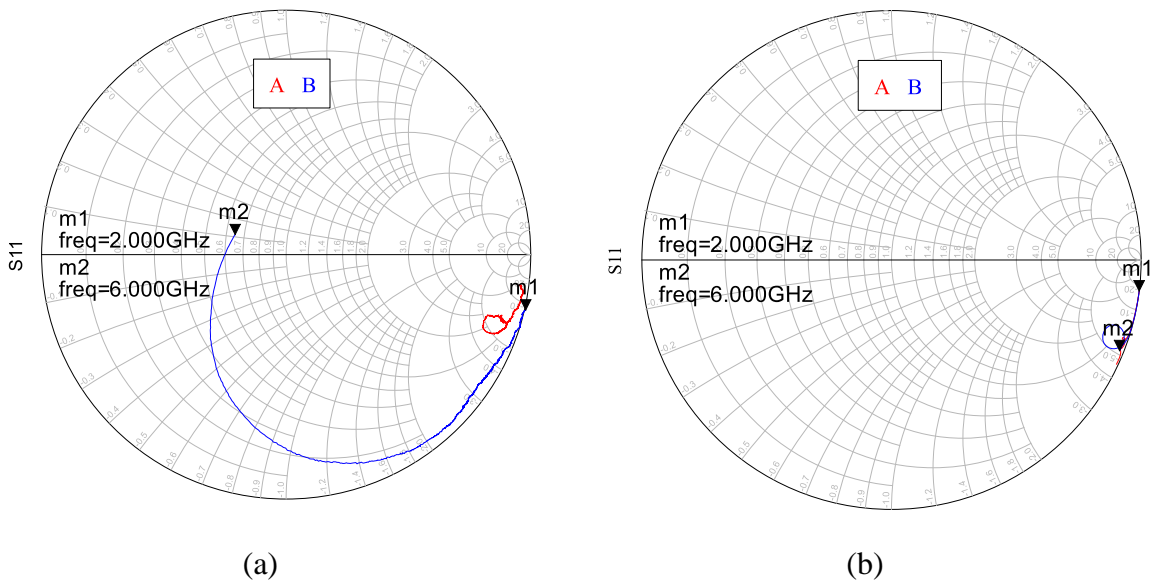


Figure 5-6 Shows the reflection coefficient (S11) for the *Original design antenna* configuration A and B. (a) shows the measured result and (b) shows the simulated results.

As seen in Figure 5-6, the measured reflection coefficient for *original design antenna* with configuration A shown in (a) is similar to the simulated one in (b). The measured reflection coefficient for *original design antenna* with configuration B is different in behaviour, the

absolute value of S_{11} decreases as the frequency increases compared to an almost constant absolute value.

5.2.2 With 50 Ohm

The reflection coefficient was measured for each of the five antennas with the resistor connected. S_{11} for the *open coax antennas* are shown in Figure 5-7 (a) and S_{11} for the *original design antennas* are shown in Figure 5-7 (b).

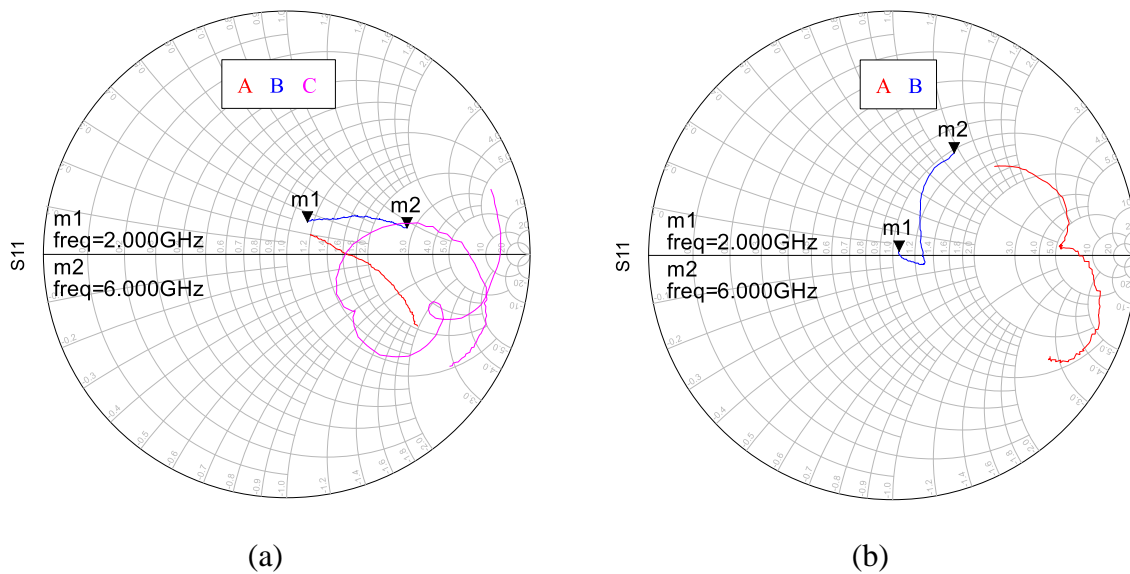


Figure 5-7 Shows measurements of reflection coefficient in a frequency sweep from 2 to 6GHz. (a) shows measurements on the *open coax antennas*, and (b) shows measurements on the *original design antennas*.

As seen in Figure 5-7, the absolute value of the reflection coefficient for all 5 antennas have been reduced drastically compared to results in section 5.2.1. In the case of the *open coax antenna* with configuration A and B, the absolute value of the reflection coefficient increases with frequency, but for configuration C, it has a minima at 3.88GHz.

5.3 Forward Loss

The Forward Loss Factor is calculated as described in chapter 2.1.4 using the values measured and shown in chapter 5.1 and 5.2.

5.3.1 Without 50 Ohm

The Forward Loss Factor was measured for all five antennas without the resistor connected. FLF is shown for the *open coax antennas* in Figure 5-8 (a) and for the *original design antennas*

in Figure 5-9 (a). The simulated Forward Loss Factor is shown for the *open coax antennas* in Figure 5-8 (b) and for the *original design antennas* in Figure 5-9 (b).

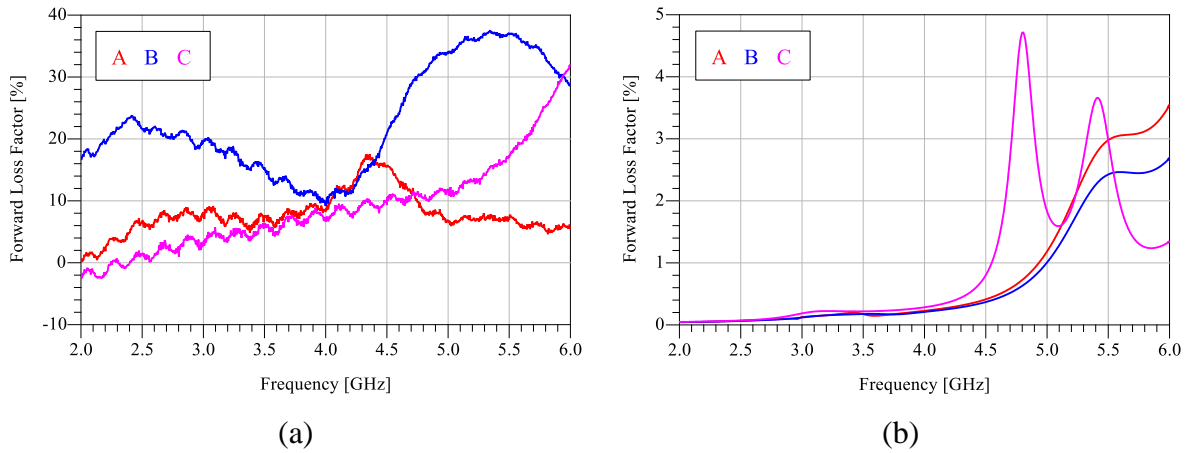


Figure 5-8 shows the Forward Loss Factor described in chapter 2.1.4 for the *open coax antenna* configuration A to C. (a) shows the measured results and (b) shows the simulated results.

It is seen in Figure 5-8, that the loss have increased over the whole frequency range. Specifically for *open coax antenna* configuration B, where the FLF is below 0.4% up to 4GHz in the simulations, but is between 10 and 25% up to 4.5GHz in the measurements. Configuration A are also increased in measurements compared to simulations

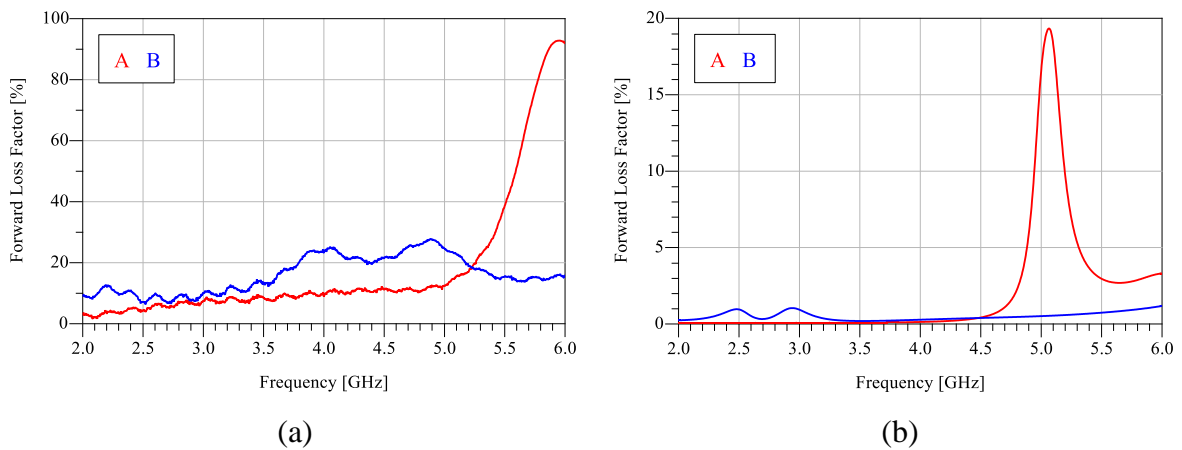
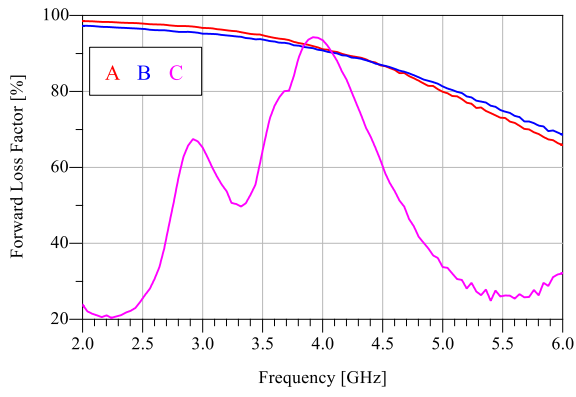


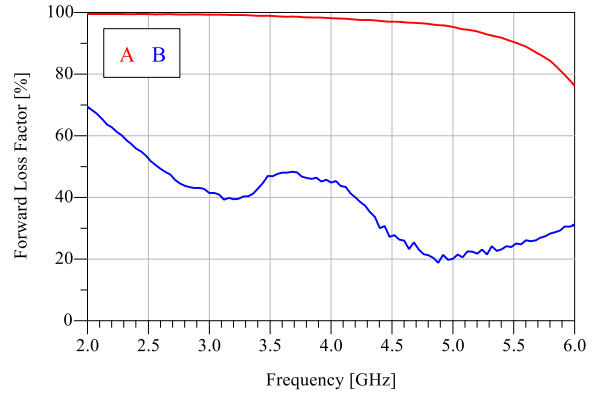
Figure 5-9 shows the Forward Loss Factor described in chapter 2.1.4 for the *original design antenna* configuration A and B. (a) shows the measured results and (b) shows the simulated results.

5.3.2 With 50 Ohm

The Forward Loss Factor where measured for each of the five antennas with the resistor connected. The FLF for the *open coax antennas* are shown in Figure 5-10 (a) and FLF for the *original design antennas* are shown in Figure 5-10 (b).



(a)



(b)

Figure 5-10 shows the Forward Loss Factor for the measurements done with the 50Ohm resistor connected to the antennas. (a) shows for the *open coax antennas* and (b) shows for the *original design antennas*.

6 Discussion

6.1 Practical issues

Some practical issues or challenges during the master's thesis are discussed here.

6.1.1 CST

It should be mentioned that a lot of the time spent during this project was spent trying to solve errors in CST. This resulted in less time for theory, which is lacking in this report. The student realizes that the simulations should have been prioritized less, and the theory should have been more in focus.

6.1.2 Standing wave

Because of miscommunication between CST and the student, the information that CST uses a 50 Ohm as matching for all antennas not just to improve transmission, but to stabilize the measurements were received late in the project. Because of the late timing, there was no time to create a CST model with the selected resistor.

6.2 Reflection coefficient

6.2.1 Wire

By inserting a resistor, more power is lost for the lower frequencies, since the resistor is 56 Ohm, it has a good match for the 50 Ohm port. The two antennas that use wire to connect the resistor, have different responses on the reflection coefficient. This is probably because of the wire that creates an inductive spurious effect. This gives the Reflection coefficient another response than the other antennas. Where the others have low absolute values because of the resistance, the two with the wire have somewhat higher absolute value of S_{11} with what would look like a resonance at several frequencies. This indicates that the use of wire for soldering of resistor was unwise, but in lack of better options, it was done. To get some more reliable measurements of the reflection coefficient, it is suggested to print a new layout with shorter paths connecting the resistor.

6.2.2 Impedance matching

To attain the best transmission possible with the antenna, impedance matching should be introduced. By using lumped components/transmission lines, it is possible to match the input impedance so that the reflected wave is smaller for a selected frequency band. Since the resistor is used to reflections over a larger frequency band, it should still be used, and additional matching could be used for the band used during transmission (2.4-2.483GHz).

6.3 Stability

The 50 Ohm resistor was used to increase stability in the measurements. During measurements without the resistor, the value of S_{21} changed up to 10dB just by the student physically touching the coaxial cable connecting the antenna. When measuring with the resistor in place, this changed up to 4dB, which still is a lot. To ensure correct measurements, the antennas should be set in a connector house. This would include some extra work, but the antennas are very dependent on their surroundings and this will give more accurate results. One could argue that this is not necessary since the variations are at 4dB, and the transmission coefficient is for instance -45dB as seen with *original design antenna* option B. Worst case then becomes -49dB, which is well above 60dB. The reason why this can not just be accepted, is that it is possible that the interference of the connector will create a notch at the used frequency band.

6.4 Transfer rate vs antenna type

All of the antennas tested have a similar behavior as the simulations, but there is a frequency offset of 1-1.5GHz for the *original design antenna*. The frequency offset is stronger represented in the *open coax antenna* with configuration C, here the offset is estimated to be 1.2GHz, which is similar to the shift for the *original design antenna*. Both antenna types need some iterations different parameters before they are optimal for transfer of the wifi-signal. These iterations should be done using the actual connectors as a measuring rig to get predictable and stable results.

7 Conclusion

This thesis presents a parametric study of both the *original design antenna* and the *open coax antennas*. Simulated, and measured results compare well except a frequency shift was observed and discussed. The stability of the measurements were increased by inserting a resistor with positive results.

To conclude, the presented antennas were usable for transmission using the wifi-chip, but further testing with the actual connector is recommended to increase the predictability and stability.

8 Further work

8.1 Connector

Further work should include testing the antennas inside the connector itself. This is to avoid any instabilities the change in surroundings may induce. This testing should be done in seawater to mimic the actual use as much as possible.

8.2 Iterations

As seen, the frequency response of the antennas may be manipulated by changing the configurations. To increase transmission, an iteration setup is recommended, where a configuration is used, and the variables are changed to control the frequency response. This could increase the stability of the connector.

Appendix A

Original design antenna

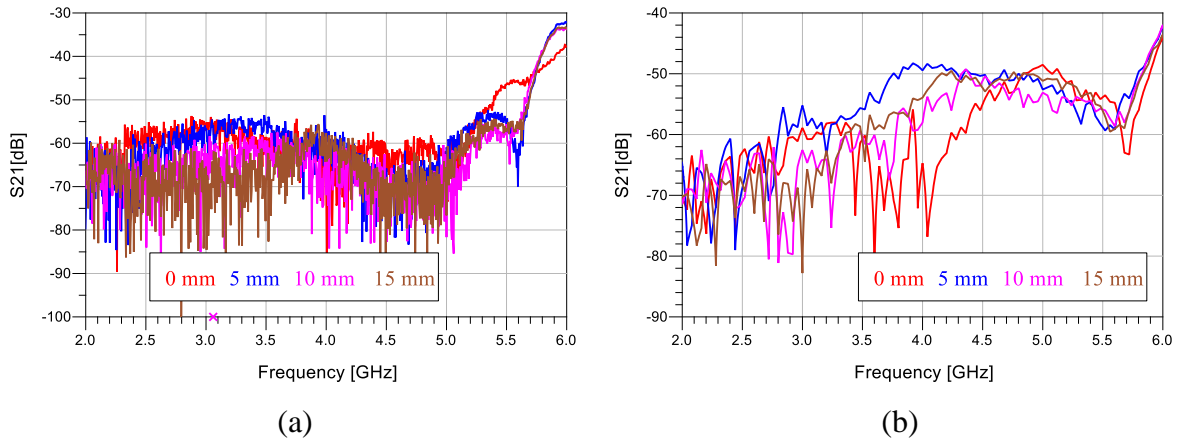


Figure 11 shows the transmission coefficient for *original design antenna* with configuration A. (a) shows with resistor connected, and (b) shows without any resistor

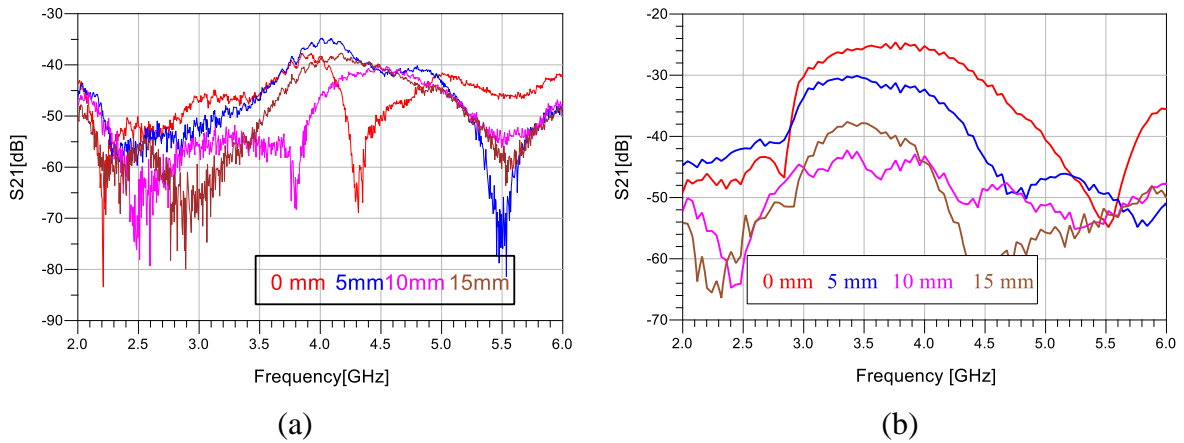
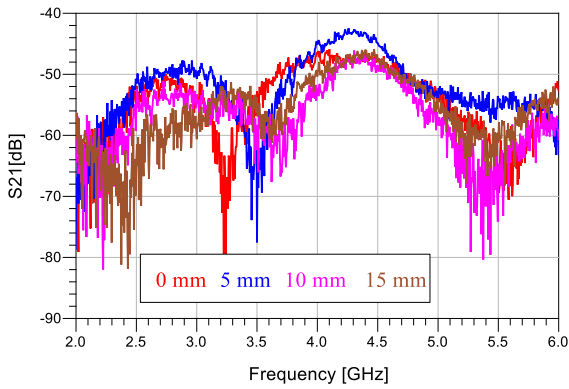
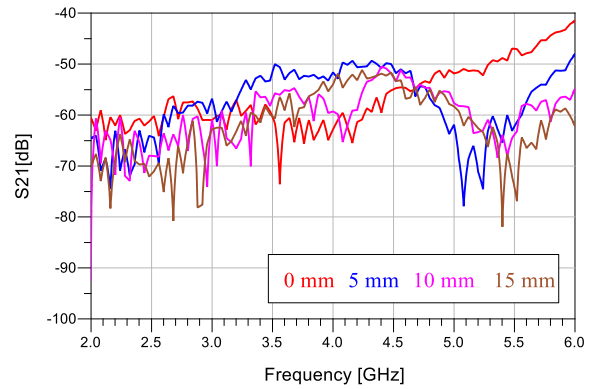


Figure 12 shows the transmission coefficient for *original design antenna* with configuration B. (a) shows with resistor connected, and (b) shows without any resistor

Open coax antenna

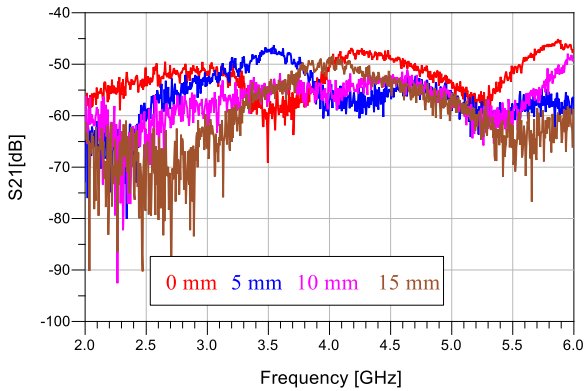


(a)

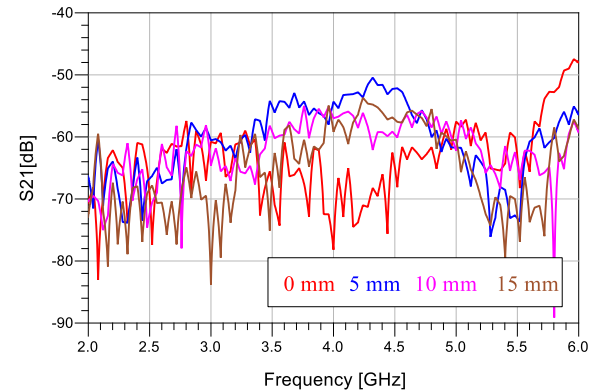


(b)

Figure 13 shows the transmission coefficient for *open coax antenna* with configuration A. (a) shows with resistor connected, and (b) shows without any resistor

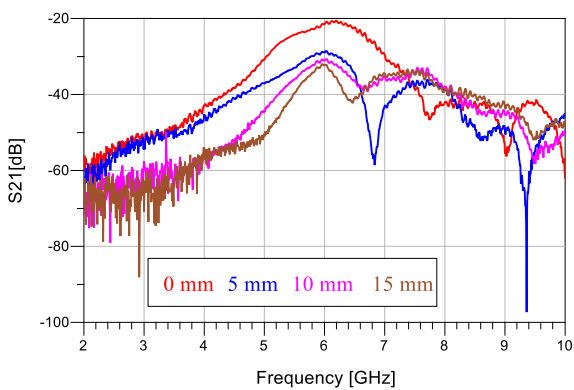


(a)

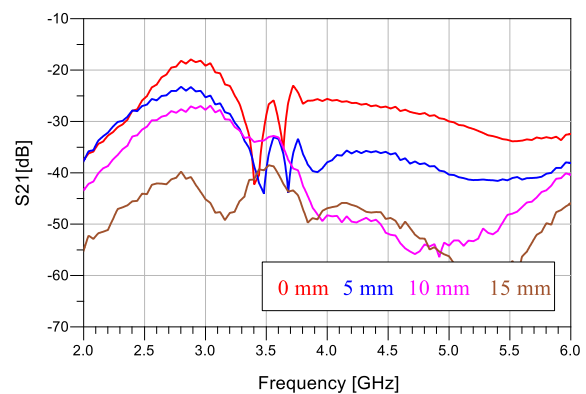


(b)

Figure 14 shows the transmission coefficient for *open coax antenna* with configuration B. (a) shows with resistor connected, and (b) shows without any resistor



(a)



(b)

Figure 15 shows the transmission coefficient for *open coax antenna* with configuration C. (a) shows with resistor connected, and (b) shows without any resistor

9 Bibliography

- [1] L. A. Larsen, "Prosjektoppgave," Norwegian University of Science and Technology, Trondheim, 2015.
- [2] Wireless Power & Communications AS, "WPC," Wireless Power & Communications, [Online]. Available: www.wpc.no. [Accessed 11 April 2016].
- [3] WIZnet, *WizFi630 User Manual*, Wiznet, 2012.
- [4] R. Schmitt, *Electromagnetics Explained*, 2002.
- [5] C. A. Balanis, *Antenna Theory Analysis and Design*, John Wiley & Sons INC, 2005.
- [6] D. K. Cheng, *Field and Wave Electromagnetics*, Pearson Education Limited, 1983.
- [7] Agilent Technologies, *Agilent AN 154 S-Parameter Design*, Agilent Technologies, 2005.
- [8] J. Capwell, T. . Weller, D. Markell and L. Dunleavy, "Automation and Real-time Verification of Passive Component S-parameter Measurements Using Loss Factor Calculations," *Microwave Journal*, 2004.
- [9] G. Breed, "Basic Principles of Electrically Small Antennas," *High Frequency Electronics*, 2007.
- [10] A. k. Bhattacharyya, "Effects of Finite Ground Plane on the Radiation Characteristics of a Circular Patch Antenna," *IEEE*, vol. 38, no. 2, pp. 152-159, 1990.
- [11] J. Watkins, "Circular Resonant Structures in Microstrip," *Electronic Letters*, vol. 5, no. 21, p. 524, 1969.
- [12] L. C. Shen, S. A. Long, M. R. Allerding and M. D. Walton, "Resonant Frequency of a Circular Disc, Printed-Circuit Antenna," *IEEE*, p. 2, 1976.
- [13] J. J. Lee, D. Charlton and W. L. Lange, "Noncontact RF connector". United States of America Patent US 5977841 A, November 1999.
- [14] K. T. McDonald, "Analysis of TEM waves in a Coaxial Cable via the Scalar Potential," Joseph Henry Laboratories, Princeton, 2010.

- [15] Teaching Science as Inquiry, "Exploring out fluid earth," [Online]. Available: <https://manoa.hawaii.edu/exploringourfluidearth/physical/density-effects/density-temperature-and-salinity/practices-science-making-simulated-seawater>. [Accessed 14 04 2016].
- [16] A. Mehta, "Microstrip Antennas," *INTERNATIONAL JOURNAL OF SCIENTIFIC & TECHNOLOGY RESEARCH*, vol. 4, no. 3, p. 3, 2015.
- [17] T. Zhang, Y. Zhang, W. Hong and K. Ku, "Wideband Millimeter-Wave SIW Cavity Backed Patch Antenna Fed by Substrate Integrated Coaxial Line," *IEEE*, p. 4, 2015.
- [18] C. Icheln, "Methods for measuring RF radiation properties of small antennas," Helsinki University of technology radio laboratory publications, Helsinki, 2001.
- [19] E. Perahia, "IEEE 802.11n Development: History, Process and Technology," *IEEE*, pp. 48-55, 2008.
- [20] D. M. Pozar, *Microwave and RF Design of Wireless Systems*, 2001.